Ocean Engineering 318 (2025) 120114

Contents lists available at ScienceDirect

Ocean Engineering

journal homepage: www.elsevier.com/locate/oceaneng

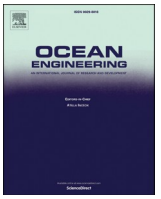

A comprehensive review of the research on local scour below subsea pipelines under steady currents and waves

Ming Zhao

School of Engineering, Design and Built Environment, Western Sydney University, Penrith, 2751, NSW, Australia

ARTICLE INFO

Keywords:
Scour
Pipeline
Sagging
Vibrating
Self-burial
Protection
Numerical method
Three-dimensional scour
Piggyback
Spoiler
Scaling effect
Machine learning

ABSTRACT

This paper presents a comprehensive review of studies of local scour below subsea pipelines. The review covers a variety of topics including onset of scour, scour depth, scour time scale, three-dimensional scour, pipeline sagging, multiple pipelines, scour protection, pipeline self-burial, scour-vibration interaction, scaling effects and cohesive sediment. Scour has been much more investigated by two-dimensional (2D) experimental and numerical studies than three-dimensional (3D). The fundamental mechanisms of 2D scour have been fully understood and many empirical formulae have been developed for predicting the scour depth under various conditions including current, waves, combined wave-current and vibrating pipelines. Some important research gaps are identified as a result of the review. 3D scour has not been sufficiently studied and more experimental data are required to support the methods that have been proposed or will be proposed. In addition, scaling effects, scour protection and self-burial have been reported but they are not sufficiently investigated.

List of Symbols

Symbol	Meaning
A_0	Amplitude of forced vibration
A^*	Non-dimensional vibration amplitude
C_p	Pressure coefficient
D	Diameter of a small pipe
d_s	Sediment particle diameter
D	Pipeline diameter
E	Pipeline material modulus
E_s	Erosion rate
E	Pipeline embedment depth
f_0	Frequency of forced vibration
f^*	Non-dimensional vibration frequency
G	Gravitational acceleration
KC	Keuleagan–Carpenter number
H	Wave height
H	Water depth
I	Pipeline section area of moment of inertia
L	Wavelength
L_{span}	Suspended free span length due to scour
n	Porosity of sand
p	Pressure
s	Specific gravity of sand
S_e	Equilibrium scour depth
S_{wc}	Scour depth under combined waves and current

(*continued on next column*)

(*continued*)

Symbol	Meaning
S_c	Scour depth under current only
S_w	Scour depth under waves only
S_f	Final sagging distance
S^*	Ratio of scour of a vibrating pipeline to non-vibrating pipeline
t	Time
t_f	Sagging duration
T_b	Time scale by Briaud et al. (1999)
T_s	Time scale of scour
T_s^*	Non-dimensional time scale of scour
R_c	Flow ratio for combined waves and current
u_0	Flow velocity above the boundary layer
U	Flow velocity in current only condition
U_c	Steady current component of velocity
U_R	Ursell number
U_{RP}	Modified Ursell number
U_w	Velocity amplitude of oscillatory flow under waves
$V_{\max}$	Maximum velocity of vibration
V_{span}	Scour propagation speed along pipeline span
V_H^*	No-dimensional scour velocity in the spanwise direction
w	Submerged weight of pipeline per unit length
x, y	Coordinates
Z_p	Sagging displacement
β	Angle of buried part of a pipeline

(*continued on next page*)

E-mail address: m.zhao@westernsydney.edu.au.

https://doi.org/10.1016/j.oceaneng.2024.120114
Received 30 September 2024; Received in revised form 28 November 2024; Accepted 13 December 2024
Available online 20 December 2024

(*continued*)

Symbol	Meaning
β_s	Sediment static repose angle
γ	Specific weight
λ_A	A coefficient for scour onset condition
θ	Shields parameter
θ_c	Critical Shields parameter
θ_p	Position angle on pipeline surface
θ_{cw}	Shields parameter under combined waves and current
τ	Shear stress
ξ	Direction along the buried PL surface

1. Introduction

Local Scour is the removal of sediment from around subsea structures on the seabed due to locally amplified water flow and it is a threat to the structural stability (Sumer and Fredsøe, 2002). The most common subsea structures are cylindrical structures in the format of vertical piles or horizontal pipelines (PLs). The mechanisms of scour around these two types of structures are different from each other. Pile scour is mainly caused by horseshoe vortex and vortex shedding, while PL scour is mainly caused by the accelerated velocity through the gap between PLs and the seabed, and vortex shedding. When a subsea PL is laid on the seabed with a small embedment depth, the seepage flow driven by the pressure gradient below the PL causes the onset of scour (Chiew, 1990; Sumer et al., 2001). Scour occurs in three-dimensional fashion as illustrated in Fig. 1. Onset of scour occurs at a weak point along the PL span where the burial depth is shallow as shown in Fig. 1 (a). After onset, the scour hole deepens and propagates in the spanwise direction. With the increase in the free span length, the PL sags into the scour hole due its own weight and finally touches the bottom of the scour hole, which is referred to as touchdown hereafter. Sagging of a PL into the scour hole for a short distance deepens the scour (Cheng and Li, 2003). After the PL sags into the scour to a critical level, the scour stops. If a PL sags into a scour hole very fast, the PL touches the seabed before the scour is fully developed, as a result, the scour depth is shallow (Draper et al., 2015). After touchdown, under the live bed condition, the sand from upstream of the PL backfills the scour hole and self-burial is illustrated in Fig. 1 (d).

Increasing number of subsea structures are being installed on the seabed with the fast development of offshore energy engineering projects, renewable or non-renewable, making the research on scour increasingly important. In ocean environment, PLs are subjects to current, waves, or combined waves and current, making it important to study the scour under all these flow conditions. Numerous studies have been conducted to understand scour processes of various kinds of subsea structures and quantify the scour depth and scour time scale.

Although the scour process is three-dimensional (3D), many studies of local scour were conducted in the two-dimensional (2D) configuration, where the PL is rigid, and scour does not vary along the span. The 2D configuration assumes the scour and flow at the centre of the free span is nearly two-dimensional. This assumption does not introduce noticeable error because the curvature of the PL is very small. It allows the scour experiments to be conducted in a 2D water flume and the numerical simulations to be conducted using 2D numerical models. After onset, scour below a PL can be divided to two stages (Bijker and Leeuwestein, 1984): tunnel scour at the early stage that is mainly dominated by the velocity acceleration through the gap, and lee wake scour that is dominated by the vortex shedding. Vortex shedding does not occur until the gap between the PL and seabed has been sufficiently large, and sufficient large scour hole has developed. The onset condition of scour, the scour depth below a PL and the evolution of the scour depth below them are the key factors to be quantified. Numerical studies have been conducted to quantify these important factors and derive practical formulae to calculate them. When 3D scour is studies, the propagation speed of the scour hole along the spanwise direction is the key factor to be evaluated (Fredsøe et al., 1988; Cheng et al., 2009).

Self-burial could be beneficial, but before the self-burial, the very long free span length can cause strong vibration caused fatigue failure of PLs (Li et al., 2021b, 2023). Vibration of suspended part above the scour of PLs is a significant hazard to PL safety. The vibration of PLs and scour mutually affect each other: scour-induced free span allows vibration to occur, and vibration enhance the scour (Gao et al., 2006; Dhamelia et al., 2023a). The hazard of scour and vibration to PLs make it necessary to protect scour from happening. Research has been conducted to protect PLs from scour and the very common method of scour protection is covering the seabed with unerodable materials like geotextile mattresses (Xie et al., 2019a), rigid/flexible plates (Yang et al., 2014; Karamzadeh et al., 2024) and solidified soils (Hu et al., 2022a).

The studies of scour around vertical piles have been summarized in several review papers (Qu et al., 2024; Tafarojnoruz et al., 2010; Liang et al., 2020; Guan et al., 2022), however, the studies of scour below subsea PLs have never been comprehensively reviewed. The book by Sumer and Fredsøe (2002) mainly reviewed research before 2000. The review by Chen and Zhang (2009) was limited to the prediction of scour depth. The review paper by Fredsøe (2016) pointed out that the improvement of numerical modelling and 3D scour needed to paid more attention in future studies. Scour below PLs has been studies extensively in recent years and it is necessary to summarize the research outcomes, identify research gaps and research opportunities in an in-depth review, which is the purpose of this paper.

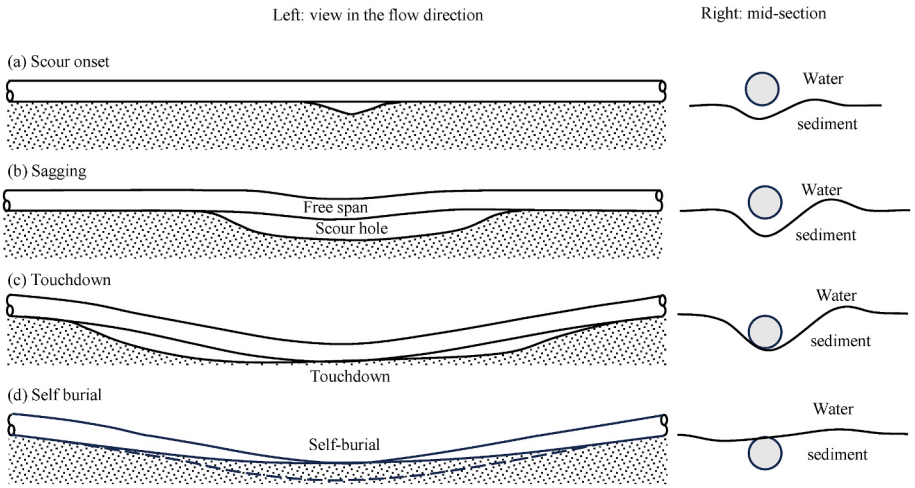

Fig. 1. Sketch of three-dimensional scour process (Fredsøe et al., 1988). Left: view in the flow direction; Right: mid-section of the free span.

This paper presents a comprehensive review of the studies of local scour below subsea PLs. Appendix shows the list of most important findings of the studies of PL scour. These findings can be classified into a variety of topics including onset of scour, scour depth, scour time scale, three-dimensional scour, PL sagging, multiple pipelines, scour protection, PL self-burial, scour-vibration interaction, scaling effects and cohesive sediment. This paper firstly summarizes the research findings of each aspect, identifies the research gaps, and then recommends future research directions. In the rest of the paper, different aspects of research on scour are reviewed in the following sections.

Section 1: Introduction section providing background of the research on scour.

Section 2: Onset of scour under current and waves.

Section 3: Scour depth and time scale prediction methods.

Section 4: 3D scour with focus on the prediction of the propagation speed of scour in the spanwise direction.

Section 5: Pipeline sagging and its effects on scour.

Section 6: The effects of multiple PLs, including piggyback PLs and two parallel PLs on the scour.

Section 7: Review of scour protection methods and their effectiveness.

Section 8: The interaction between scour and vibration.

Section 9: Prediction of local scour including numerical models and machine learning.

Section 10: Scaling effect.

Section 11: Cohesive sediment.

Section 12: Conclusions and discussions.

2. Onset of scour

When a PL with a diameter of D is laid on a sediment bed with an embedment depth e as shown in Fig. 2 (a), scour occurs when the e/D is sufficiently small and the onset of the scour is caused by the seepage flow driven by the pressure difference between the upstream point A and downstream point B (Chiew, 1990). This pressure difference is correlated to the flow velocity, the burial depth of the PL and the sediment properties. Under the wave condition, the onset condition is also affected by Keuleagan–Carpenter (KC) number defined by $KC = U_w T/D$, where U_w is the amplitude of the oscillatory flow velocity under waves on the seabed level and T is the period of the waves. Based on the experimental method, Sumer et al. (2001) proposed a criteria to determine the onset of scour for steady currents:

$$\frac{1}{\gamma}\frac{\partial p}{\partial \xi} \geq (s-1)(1-n) \tag{1}$$

where p is the pressure, γ is the specific weight of the water, ξ is the direction along the PL surface defined in Fig. 2 (a). Assuming the pressure is linearly distributed along buried surface of the PL, the pressure gradient is (Sumer et al., 2001):

$$\frac{\partial}{\partial \xi}\left(\frac{p}{\gamma}\right) = \frac{p_A - p_B}{\gamma \widehat{AB}} \tag{2}$$

where $\widehat{AB}$ is the arc length between A and B. Fig. 2 (b) shows the evolution of the pressure difference between A and B when the velocity increases gradually measured in the experiment (Sumer et al., 2001) and numerical simulation (Tsai et al., 2022), where the time is non-dimensionalized by t_p, which is the time when the pressure difference $\frac{p_A - p_B}{\gamma \widehat{AB}}$ reaches its maximum value before dropping. When the flow velocity is increased to a critical value, the seepage flow is so strong that the sand-water mixture break through the space underneath the PL, and this phenomenon is referred to as piping. Piping is the main mechanism responsible for the onset of scour below pipelines.

Zang et al. (2009) investigated onset of scour by calculating the pressure distribution in the water and sand through CFD simulations. They found that onset of scour happens when:

$$\frac{u_0^2}{gD(s-1)(1-n)} \geq \frac{\beta}{\lambda_A \Delta C_{p0}} \tag{3}$$

where u_0 is the free-stream velocity, g is the gravitational acceleration, D is the diameter of the PL, β is the angle defined in Fig. 2 (a), $\Delta C_{p0} = C_{p0,A} - C_{p0,B}$, where $C_{p0,A}$ and $C_{p0,B}$ are the pressure coefficient at points A and B, respectively, $C_{p0} = \frac{p - p_0}{\rho u_0^2/2}$ is the pressure coefficient, and λ_A is a coefficient fitted based on the experimental data. ΔC_{p0} was found to be weakly dependent on the Reynolds number, but significantly affected by the water depth and boundary layer thickness. The coefficient λ_A is nearly independent on the water depth but is a function of angle β that is correlated to embedment depth:

$$\lambda_A = 3.0 \exp(-0.42\beta) \tag{4}$$

The critical flow velocity for scour onset to occur can be then calculated based on Eq. (3). Zhang et al. (2014) investigated onset of scour numerically using CFD-DEM coupled method. The numerical results of the critical velocity agree well with others in Fig. 3. The onset of the scour can be straightforwardly visualized by CFD-DEM solution as DEM can resolve the granular medium at the particle scale and simulate particle-to-particle interaction.

The above-mentioned onset conditions of scour are valid for the case where a PL is placed on a large area of seabed fully covered by sand bed. If the PL is under an environment where insufficient supply of sand is available from the upstream, onset occur under lower current velocity or smaller embedment depth (Zhang et al., 2016a). This implies that scour could occur under deeply embedded pipelines on sand bed with unerodable bed upstream. Onset can also occur earlier under conditions with field irregularities caused by for example field joints (Griffiths et al.,

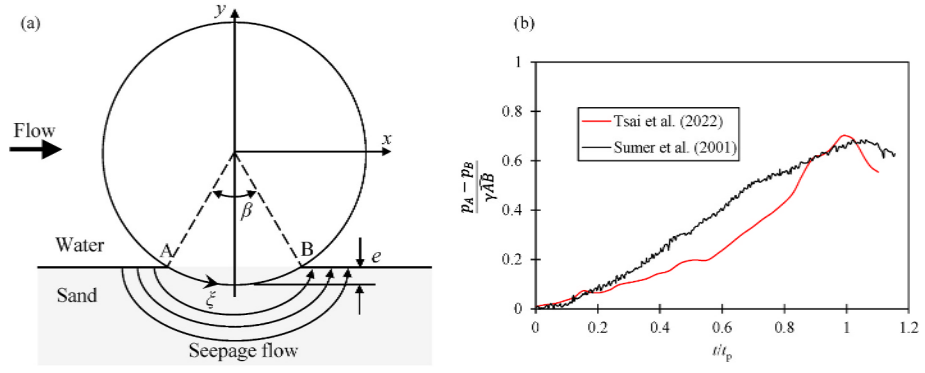

Fig. 2. (a) Seepage flow beneath a pipeline with an embedment depth e; (b) The evolution of the pressure difference between when the flow velocity increases with time.

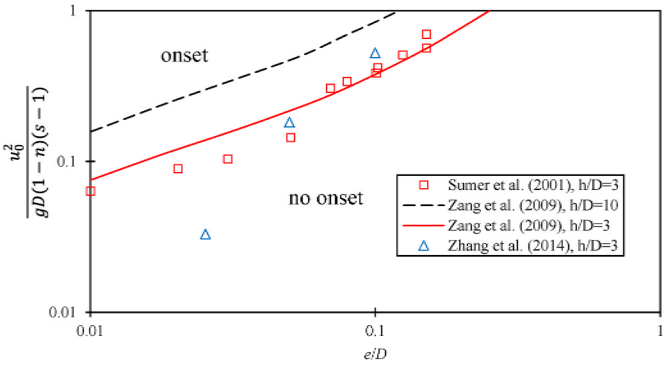

Fig. 3. Compare between the scour onset conditions under steady current from different studies.

2016).

When onset of scour under waves was investigated, it was reported that when the pressure meets the onset condition, the onset of scour occurs after several wave periods instead of immediately after waves act on the PL. The reason why onset is delayed is because the exposure time of the sand to high pressure gradient is short in one wave period and it require several wave periods to allow the piping to take place. This development of piping over multiple wave periods was also captured by scour onset visualization recorded by camera (Zhu et al., 2020b). Through visualization, Zhu et al. (2020b) reported that oscillatory motion of sand initiated at the downstream point B and extends towards the upstream point A before piping occurs. Sumer et al. (2001) and Zang et al. (2009) measured and numerically calculated the onset condition, respectively. By modifying Eq. (3), Zang et al. (2009) proposed an empirical formula for predict the onset condition under waves:

$$\frac{U_w^2}{gD(s-1)(1-n)} \geq \frac{\beta}{\lambda_A \Delta C_{p0}}\left[1-\exp\left(-0.018KC^{1.5}\right)\right] \tag{5}$$

where ΔC_{p0} is the pressure coefficient under the current condition. Eq. (5) following similar format as Eq. (3) for steady current but with a modification term of $1-\exp\left(-0.018KC^{1.5}\right)$. The empirical formula Eq. (5), the numerical results and the measured data are compared with each other in Fig. 4. The measured data are very scattered even when the axes are the logarithmic scale, mainly because they are from a wide range of KC numbers. The empirical formula agrees well with the numerical results and qualitative well with the measured data.

3. Scour depth and time scale

Many studies have been conducted in two-dimensional (configurations), where the PLs were rigid, and the scour does not vary along the PL, and this type of scour is referred to as 2D scour. 2D The scour represents the scour process of the mid-section of the free span of a rigid PL shown in Fig. 1. Scour depth below a PL and time scale are the most important factors that need to be evaluated in 2D scour. The scour speed is evaluated by time scale that will be defined in section 3.2.

Under steady current condition, both scour depth and time scale are determined by the Shields parameter (θ) defined as:

$$\theta = \frac{\tau}{(s-1)\rho g d_s} \tag{6}$$

where τ is the bed shear stress caused by the flow, d_s is the sediment particle size, ρ is the density of the water and g is the gravitational acceleration. Under wave condition, the scour depth is mainly affected by the KC number in the live bed condition. Under the combined waves and current, the scour depth is also affected by the velocity ratio between waves and current in addition to the KC number. The velocity ratio R_c is defined as:

$$R_c = U_c / (U_c + U_w) \tag{7}$$

where U_c and U_w are the velocity of steady current and velocity amplitude of the oscillatory flow under waves, respectively.

3.1. Equilibrium scour depth

After the onset of scour, the scour profile changes fast initially, the change rate decreases with time and finally reaches an equilibrium stage. The equilibrium scour depth below the PL under steady current is (Kjeldsen et al., 1973):

$$S_e = 0.972\left(\frac{U^2}{2g}\right)^{0.2} D^{0.8} \tag{8}$$

where S_e is the equilibrium scour depth, U is the steady current velocity. As the Shields parameter is linearly proportional to U^2, the above equation indicates that S_e varies with θ by a power of 0.2, and this variation is very weak (Sumer and Fredsøe, 1990).

Under waves, the equilibrium scour depth is related to the KC number (Sumer and Fredsøe, 1990; Sumer and Fredsøe, 1990):

$$\frac{S_e}{D} = 0.1\sqrt{KC} \tag{9}$$

Based on the least square method Çevik and Yüksel (1999) derived a formula in the similar format:

$$\frac{S_e}{D} = 0.11(KC)^{0.45} \tag{10}$$

Instead of using Eq. (8), Çevik and Yüksel (1999) recommend using the Ursell number to calculate wave-induced equilibrium scour depth:

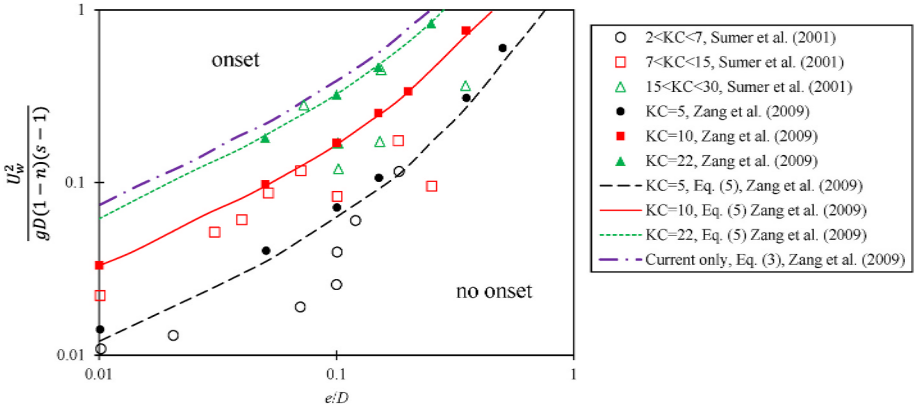

Fig. 4. Compare between the scour onset conditions under waves from different studies.

$$\frac{S_e}{D}=0.042U_{RP}^{0.41} \tag{11}$$

where the modified Ursell number $U_{RP}=U_R\left(\frac{H}{D}\right)^2=\frac{H^3L^2}{h^3D^2}$, and the Ursell number $U_R=\frac{HL^2}{h^3}$, h is the water depth and L is the wave length. The modified Ursell number includes the local wave height, the local wavelength, the local water depth, and the PL diameter. The correlation between the relative scour depth and U_{RP} is high for both slope and horizontal bed.

The above formulae did not consider the effect of the Shields number as it was derived based on the experimental data under the live bed condition. When the bed material is coarse and scour is under clear-water condition, the scour depth will be reduced compared with live-bed scour (Vosoughi and Hajikandi, 2020; Dogan et al., 2018). Dogan et al. (2018) developed a formula for wave-induced scour depth under clear water condition:

$$\frac{S_e}{D}=0.001(KC)^2 \tag{12}$$

Fig. 5 shows the Comparison between the experimental data (symbols) and the empirical formula for wave-induced scour. The empirical formulae from (Sumer and Fredsøe, 1990; Çevik and Yüksel, 1999) are different from each other when KC is either large or small. The scour depth of clear-water scour is apparently smaller than the live-bed. The empirical formula for clear-water condition by Dogan et al. (2018) predicts the scour depth well for in the range of KC where they measured the scour, but overestimates the scour depth at the large KC numbers (KC > 20).

Under the combined waves and current, the scour depth is affected by the flow ratio. Sumer and Fredsøe (1996) developed an empirical formula to predict the equilibrium scour depth in combined waves and current:

$$\frac{S_e}{D}=\frac{S_{e,c}}{D}F \tag{13}$$

where $S_{e,c}$ is the scour depth under currently only. Sumer and Fredsøe (1996) suggested $\frac{S_{e,c}}{D}\approx 0.6\pm 0.1$. The coefficient F is calculated by:

$$F=\begin{cases}\frac{5}{3}(KC)^a\exp(2.3b), & 0\le R_c\le 0.7\\ 1, & 0.7\le R_c\le 1\end{cases} \tag{14}$$

The coefficient a and b in the above equation is calculated by:

$$a=\begin{cases}0.557-0.912(R_c-0.25)^2, 0\le R_c\le 0.4\\ -2.14R_c+1.46, 0.4<R_c\le 0.7\end{cases} \tag{15}$$

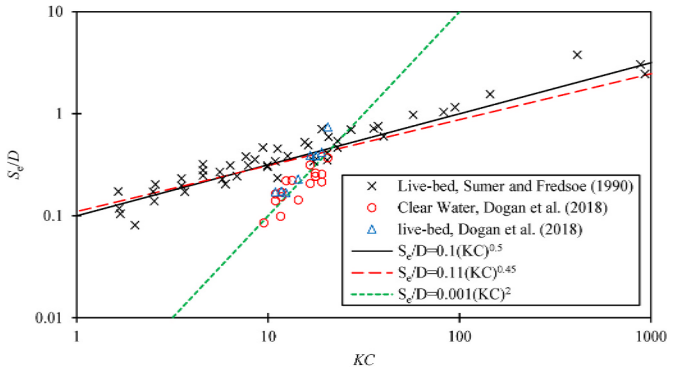

Fig. 5. Comparison between the experimental data (symbols) and the empirical formulae (lines) for wave-induced scour.

$$b=\begin{cases}-1.14+2.24(R_c-0.25)^2, 0\le R_c\le 0.4\\ 3.3R_c-2.5, 0.4<R_c\le 0.7\end{cases} \tag{16}$$

Zhang et al. (2017a) considered additional experimental data that they obtained and proposed a simpler formula for predicting equilibrium scour depth under wave and currents:

$$S_{wc}=\left(S_c^2+S_w^2\right)^{0.5} \tag{17}$$

where S_{wc}, S_c, and S_w are the scour depth under combined wave-current, current only and wave only conditions, respectively. S_w in Eq. (17) is calcualted by the formula for wave only case Eq. (9).

3.2. Time scale and scour history

The scour rate in the tunnel scour stage and decreases with time and finally reaches zero at the equilibrium stage. Fredsøe et al. (1992) proposed the first empirical formula for predicting the history of the scour depth below a PL:

$$\frac{S}{S_e}=1-\exp\left(-\frac{t}{T_s}\right) \tag{18}$$

where T_s is defined as the time scale of scour. The nondimensional time scale is defined as:

$$T_s^*=\frac{\left[g(s-1)d^3\right]^{1/2}}{D^2}T_s \tag{19}$$

and it is a function of the Shields parameter for both steady current and waves:

$$T_s^*=0.02\theta^{-5/3} \tag{20}$$

A genetic formula for predicting the history of the scour for pipelines and pile can be written as (Cheng et al., 2016):

$$\frac{S}{S_e}=1-\exp\left[-C_s\left(\frac{t}{T_s}\right)^{n_s}\right] \tag{21}$$

where the two coefficients C_s and n_s are introduced to control the evolution speed of the scour rate. Eq. (21) has been used in many studies of bridge pier scour with varies sets of coefficients (Cheng et al., 2016). Zhang et al. (2017a) conducted a comprehensive experimental study for scour under both steady current and waves and recommended $C_s=1$ and $n_s=0.6$. Then Eq. (21) becomes

$$\frac{S}{S_e}=1-\exp\left[-\left(\frac{t}{T_{s,z}}\right)^{0.6}\right] \tag{22}$$

The non-dimensional time scale is related to the Shields parameter by:

$$T_{s,z}^*=0.02\theta^{-1.5} \tag{23}$$

under the wave condition the Shields parameter θ is replaced by the maximum Shields parameters $\theta_{\max}$ in Eq. (23) (Zhang et al., 2017a). The empirical formula for scour history by Briaud et al. (1999) initially developed for bridge piers was also suitable for PLs and this formula is:

$$\frac{S}{S_e}=\frac{t}{T_b+t} \tag{24}$$

Fig. 6 shows the comparison between the above three formulae: Eq. (18), Eq. (22) and Eq. (24) for predicting scour history. The underestimation of the scour depth at the early stage by Eq. (4) was noticed by (Zhang et al., 2017a) before they derived Eq. (22). Eq. (24) and Eq. (22) performs equally well at the early stage but it appears that Eq. (22) is closer to the experimental data at the late stage.

When a PL is connected to a floating structure like a steel catenary

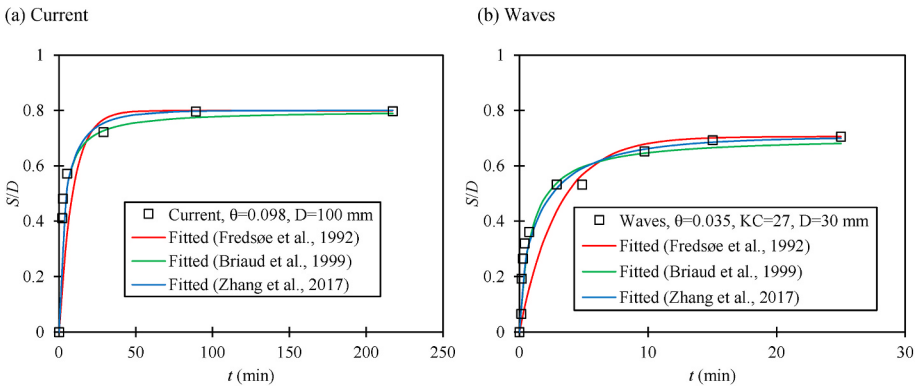

Fig. 6. Comparison between the tree formulae for predicting the time history of scour under (a) Steady current and (b) Waves. The experimental data are from (Fredsøe et al., 1992).

riser (SCR), its vibration is forced vibration driven by the motion of the structure. Zhang et al. (2022c, 2023) conducted experiments of scour of a PL with forced vibration in steady current and derived empirical formulae for predicting equilibrium scour depth and time scale using the data of clear water scour. The equilibrium scour depth is:

$$\frac{S_e}{D} = 1.068\cosh\left(0.875\frac{A_0}{D}\right)\cosh\left(15.275\frac{f_0 D}{u_0}\right)\left(\frac{\theta}{\theta_c}\right)^{1.2544} + 0.094 \quad (25)$$

where A_0 and f_0 are the amplitude and frequency of the forced vibration, respectively and u_0 is the flow velocity on the top of the boundary layer flow. The time history of a forced vibrating PL follows the genetic formula Eq. (21), but all the coefficients T_s, C_s and n_s varies with the flow and PL conditions:

$$C_s = 1.063 V_{max}^{0.263}\left(\frac{\theta}{\theta_{cr}}\right)^{0.131} \quad (26)$$

$$n_s = 0.0921\cosh\left(1.382\frac{A_0}{D}\right)\cosh\left(1.673\frac{f_0 D}{u_0}\right) \quad (27)$$

$$T_s^* = 2536.13 V_{max}^{0.465}\left(\frac{\theta}{\theta_{cr}}\right)^{1.436} \quad (28)$$

where V_{max} is the maximum velocity of the vibrating PL. It should be noted that Eqs. (26)–(28) were derived using the data of clear water scour where the PL vibrates with one-degree-of-freedom in the vertical direction. The validity of them should be checked when they are applied to a PL with two-degree-of-freedom vibration or live-bed scour. No studies of scour of PLs with forced vibration has been conducted under the live-bed condition.

4. Three-dimensional (3D) scour propagation

Scour always occurs in a three-dimensional (3D) fashion in the ocean. Onset of scour often occurs at weak points along the PL route as illustrated in Fig. 1 (a). Once scour starts, the PL goes through sagging, and self-burial stages (Fredsøe et al., 1988). When the free-span length of the PL on a scour hole is sufficiently long, the PL sags into the scour hole and touches the sand surface at the middle of the free span, and this phenomenon is called touchdown. Once the PL touches down the bottom, the scour stops and if the bed is live-bed, sand will be back-filled into the scour hole resulting in self-burial as seen in Fig. 1 (d). Based on the mechanical properties of the PL, the sagging distance of the centre point of the free-span the minimum free-span length for touchdown to occur can be calculated (Fredsøe et al., 1988; Ajdehak et al., 2018). The 3D scour process illustrated in Fig. 1 is dominated by the propagation speed V_{span} of the scour along the spanwise direction defined in Fig. 7.

Most of the studies of 3D scour used rigid PLs to investigate the mechanisms of propagation of scour hole in the spanwise direction and quantify the speed of scour propagation. Cheng et al. (2009) conducted

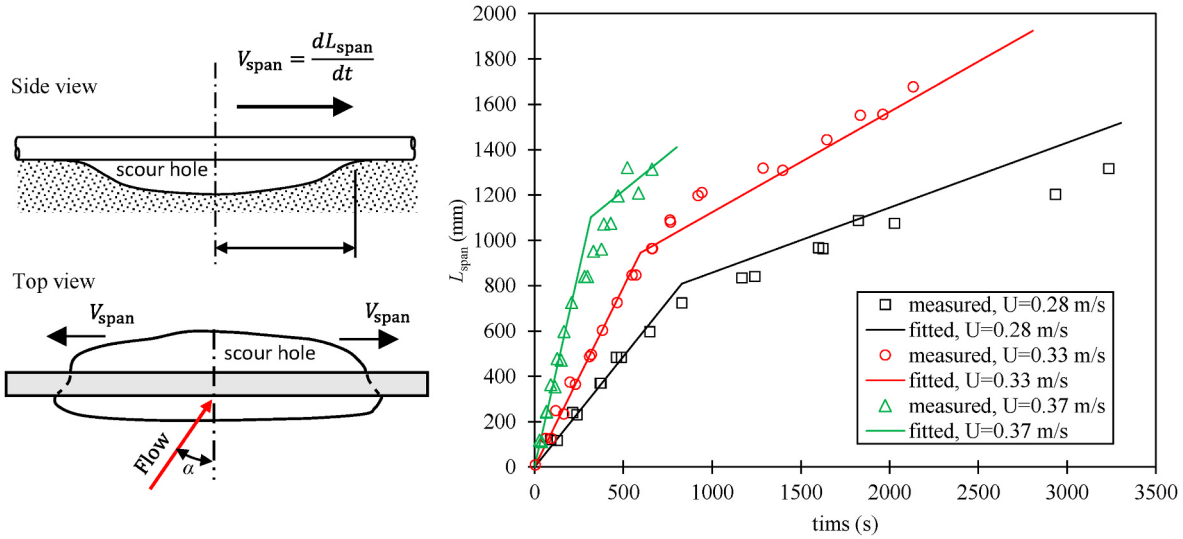

Fig. 7. Evolution of the free-span length L_{span} in 3D scour experiments of a PL D = 50 mm in steady current at α = 0° (Cheng et al., 2009). The flow direction is perpendicular to the pipeline.

experiments of a 50-mm diameter PL in a 4-m wide wave flume. Fig. 7 show the evolution of the measured free span length L_{span} with time, which is found to increase faster in the early stage (stage I) than late stage (stage II). L_{span} is a linear function of time in both stages. The empirical formulae proposed for predicting the speed of propagation in both states is (Cheng et al., 2009):

$$V_{span}=\frac{dL_{span}}{dt}=K_{span}\left(25\frac{\sqrt{g(s-1)d_s^3}}{D\tan(\beta_s)}\right)\theta^{\frac{5}{3}}\left(1-\frac{e}{D}\right) \tag{29}$$

where β_s is the static repose angle of the sand, and the constant $K_{span}=1$ 4 and 4 in stages I and II, respectively. If the PL is not perpendicular to the direction of the current, the above equation is modified to consider the influence from the angle of attack α:

$$V_{span}=\frac{dL_{span}}{dt}=K_{span}\left(25\frac{\sqrt{g(s-1)d_s^3}}{D\tan(\beta_s)}\right)\theta^{\frac{5}{3}}\left[1-\frac{e}{D}(1+\sin\alpha)\right] \tag{30}$$

where the angle of attack α is 0° when the flow is perpendicular to the PL and ±90° when the flow is parallel to the PL (see Fig. 7 for the definition of α). The above formula is derived based on the experimental data for α = 0°–45°. When the flow approaches a PL at an oblique angle, the speed on one side is slower and another side is faster. A negative α one side and a positive α on another side can be put into the above formula to calculate the speeds of the two sides, respectively. The fitted lines based on Eq. (29) at $\alpha=0°$ are compared with the measured data in experiments in Fig. 7. The proposed formula agrees well with the experimental data. As per Fig. 7, the free span length in stage I is short, its maximum value is about 1100 mm, which is about 22 diameters for a 50-mm diameter PL model. Considering the long length of a real PL, most of the time the scour process is in phase II during the scour. The maximum span length L_{span} in stage I appears to increase with the increase of the flow velocity, but no formula was given for the maximum L_{span} in stage I.

Wu and Chiew (2012) conducted further experiments on 3D scour of a PL with various water depths, current velocities, and PL diameters under clear-water condition with $\alpha=0°$. They reported that the scour process includes a rapid phase with a constant and fast scour speed, followed by a slack phase with a slower and reducing scour speed. This observation agreed with the observation by Cheng et al. (2009). The scour speed is only the function of θ in Eq. (29), but Wu and Chiew (2012) observed that V_{span}/U is dependent on F_r more than θ based on the observation in Fig. 8. They non-dimensionalized the scour depth in the rapid phase by the depth average flow velocity U and plotted it against the Froude number in Fig. 8, where U and h are the depth-averaged velocity and water depth, respectively, and the Froude number is defined as $F_r=\frac{U}{\sqrt{gh}}$. It is clear that V_{span}/U is nearly a linear function of F_r in Fig. 8. Wu and Chiew (2012) observed the scour speed in the slack phase decreases with time, instead of being constant as observed by Cheng et al. (2009).

Wu and Chiew (2013) conducted flow visualization near the shoulders of the free span using an Acoustic Doppler Velocimeter (ADV) and concluded that the increasingly concentrated and strong flow force at the span shoulder mobilize and remove the sediment after the onset of scour. Wu and Chiew (2015) further concluded that the differential pressure and the local bed shear stress at the span shoulder are responsible for the propagation of the 3D PL scour hole in the spanwise direction, however the local bed shear stress is difficult to measure and quantify in the experiments. The sediment motion near the span shoulders is strong during the rapid phase due to the small gap between the PL and sand surface and slow during the slack phase.

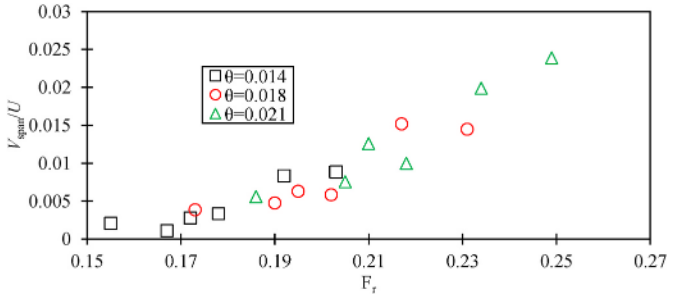

Fig. 8. Variation of V_{span}/U in the rapid phase with the Froude number (e/D = 0.1 and h/D = 4.08) (Wu and Chiew, 2012).

The difference between the experimental observation in the slack phase by Wu and Chiew (2012) and Phase II by (Cheng et al., 2009) is likely because the two studies are in clear-water and live-bed conditions, respectively. Sui et al. (2021) conducted experiments of 3D scour using a water flume with a width of 4 m, same width as that used by Cheng et al. (2009), PL diameters of 40 mm and 80 mm under live-bed condition. The reported the same two phases of scour as Cheng et al. (2009), i.e., stage I with fast scour and stage II with slow scour. The found that scour speed is correlated to the Shields parameter rather than the Froude number. However, their experimental data does not following the formula by Cheng et al. (2009) well. They found a good correlation between the scour speed in the spanwise direction and to $\theta-\theta_c$ instead of θ. The proposed the following empirical formula by Sui et al. (2021) is:

$$\frac{V_{span}}{\sqrt{g(s-1)d_s}}\cdot\frac{D}{d_s}=A\cdot\left[1+200(\theta-\theta_c)^{3/2}\right]\cdot\exp\left(-B\frac{e}{D}\right)\ for\ \theta>\theta_c \tag{31}$$

where the parameters $A=3$ and $B=3.2$ and 5 in stages I and II, respectively.

To explain the scour process, Xie et al. (2019b) visualized the evolution of geometry of the span shoulders during the scour process, which is asymmetric. A frontal angle α_f is defined in Fig. 9 to quantify the geometric asymmetry of the shoulder. They found that the front angle is initially very large and gradually reduces with time as shown on the left side of Fig. 9. During the time from t_1 to t_3 in Fig. 9, the increase of α_f can be seen. In addition to the small gap at the early stage, the larger front angle makes the scour hole in a contracted shape in the top view, and this further contributes the flow acceleration and fast scour speed in stage I. In late stage II, the front angle decreases, as a result the enhancement of the scour due to the flow contraction weakens.

Cheng et al. (2014) conducted experiments of scour of a PL under combined waves and currents. The scour propagation rate first decreases with the increase of the flow ratio R_c until $R_c\approx0.6$, then it starts to increase thereafter. They extended their formula proposed for steady current (Cheng et al., 2009) into wave-current case:

$$V_{span}=K_{wc}\left[1-\frac{e}{D}(1+\sin\alpha)\right]\left(\frac{\sqrt{g(s-1)d_s^3}}{D\tan(\beta_s)}\right)[(1-R_c)\theta_w+R_c\theta_c]^{\frac{5}{3}}F \tag{32}$$

where θ_c and θ_w are the Sheilds parameters due to current and waves, respectively, $K_{wc}=148$ and the coefficient F is calculated by Eq. (14).

The three-dimensional scour process has been rarely studied using numerical simulation because huge amount and unaffordable (for a very long PL) computational time involved. Cheng and Zhao (2010) conducted numerical simulations of 3D scour of a PL with a length of 20 diameters. Because of the short PL length, only the scour speed V_{span} in the fast scour stage I was predicted numerically, and it is about 50% lower than the measured. The numerical results proved that the high Shields parameter and the steep bed slopes at the two shoulders of the span contribute to the sediment transport and scour propagation in the spanwise direction. Numerical methods were used to investigate some problems of 3D scour that do not involve affordable amount of computational time. For examples Liang et al. (2022) numerically simulated the scour of a PL with finite length up to 6 diameters and reported that the equilibrium scour depth increased with the increase of

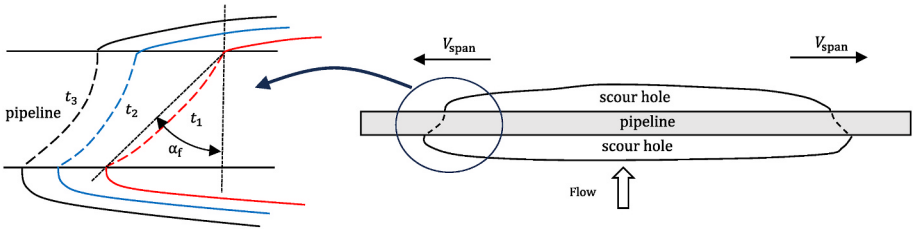

Fig. 9. Top view of the front angle at a span shoulder defined by (Xie et al., 2019b).

PL length until the latter exceeds 4 diameters. Zhang et al. (2022a) simulated scour of two PLs that cross with each other and investigated the angle of attack of the flow on the scour.

The scour-sagging-self-burial process of a real flexible PL illustrated in Fig. 1 has never been comprehensively investigated either experimentally or numerically using three-dimensional models. Some simplified 2D models were proposed to predict the process. When Ajdehak et al. (2018) simulated touchdown of the PL at the mid-section of the free-span, they used a 2D model that assumed the scour in the mid-section is two-dimensional. In this 2D model, the free-span length was predicted by empirical formula Eq. (29) and the sagging distance at the mid-section is predicted by solving the beam equation with the end condition recommended by Draper et al. (2015). Similarly, Luo et al. (2014) used the combination of 2D experiments of scour of a sagging PL and empirical formulae for predicting scour extension in the spanwise direction to predict the sagging behaviour of a flexible PL.

5. Pipeline sagging

When scour develops in a 3D fashion, PL sagging is a 3D problem as illustrated in Fig. 1. Because the scour at the centre part of the free span is close to a 2D problem and the inability of both experimental method and numerical method of studying long PLs, PL sagging has been mainly investigated using 2D experiments or 2D numerical simulations. Sagging can cause the scour depth to increase if its speed is slow to allow scour to fully develop. However, if the sagging speed is faster than the scour rate, the touchdown of the PL can cause the scour to cease before it reaches it equilibrium stage. Cheng and Li (2003) simulated scour of a sagging PL with a constant sagging speed using CFD and proved that a very small sagging speed can significantly increase the scour depth. The scour depth reaches its maximum when around half of PL is under the original seabed level with a small sagging speed.

Fredsøe et al. (1988) suggested that the sagging displacement of the free span of a PL can be calculated by:

$$Z_p = \frac{3}{384}\frac{wL_{span}^4}{EI} \tag{33}$$

where E and I are the modulus of elasticity and the area of moment of inertia, respectively, and w is the PL submerged weight per unit length.

Based on the free span length L_{span} calculated by the free span propagation speed Eq. (29), the sagging distance at the centre of the free span can be calculated using Eq. (33) and this sagging distance can be used in 2D studies to find out the scour under sagging condition. Draper et al. (2015) conducted 2D experiments to represent sagging of the centre of the free span caused by 3D scour, letting the PL sagging following Eq. (33) and calculating L_{span} based on empirical formula by Cheng et al. (2009). The experiments were conducted until the PL toughed the seabed. Fig. 10 shows an exemplar case showing how the scour depth and the sagging distance of a PL evolves. At about 30 min after the scour started, the scour depth (S_0/D) increases much faster than the sagging distance of the PL (Z_p/D) initially. At about 65 min, the sagging speed of the PL starts to increase quickly and finally surpasses the speed of scour. Finally, the sagging distance and the scour depth are the same, the PL touched the bottom and the scour stops.

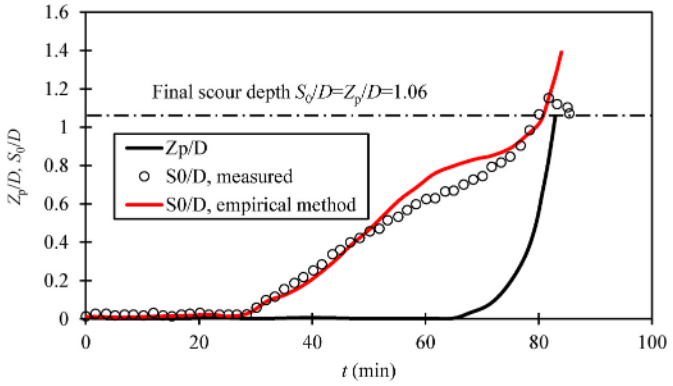

Fig. 10. Variation of the non-dimensional scour depth and the sagging distance with time in the experiment in Draper et al. (2015).

Luo et al. (2014) used similar method to experimentally predict PL sagging due to scour in waves. Ajdehak et al. (2018) continued the work of Draper et al. (2015) using a numerical method and produced the same sagging and scour process shown in Fig. 10. They conducted comprehensive numerical simulations with various PL weight, PL diameters and flow velocities. Heavy PLs touch the seabed faster than light PLs, and a same PL touch the seabed faster when flow velocity is higher. Slower the sagging speed, the deeper scour depth because the sufficient time is given to the scour to fully develop. Using the numerical data, they proposed an empirical method to predict the final sagging distance at the time when PL touches the scour hole:

$$\frac{S_f}{D} = -0.03\exp(3\theta)\log\left(16w^* V_H^{*4}\right) + 0.168\ln(\theta) + 1.275 \tag{34}$$

where the non-dimensional scour velocity in the spanwise direction is defined as:

$$V_H^* = 25K_{\text{span}}\frac{\theta^{5/3}}{\tan(\beta_s)}\left(1-\frac{e}{D}\right) \tag{35}$$

$K_{\text{span}} = 1$ 4 and 4 in stages I and II, respectively, S_f is the final sagging distance, the non-dimensional scour propagation speed in the spanwise direction is calculated by Eq. (29). The empirical formula for predicting the time (t_f) of the whole scour and sagging process from the onset of scour and until the PL touches the bottom of the scour hole by Ajdehak et al. (2018) is:

$$\frac{t_f}{T_a} = 0.993\exp\left[-0.558\log\left(C^* 16w^* V_H^{*4}\right)\right] \tag{36}$$

where $T_a = \frac{D^2}{\sqrt{g(s-1)d_s^3}}$.

When Eqs. (34) and (36) were derived, the sagging of PLs was caused by the PL's weight only. However, on a scoured bed, it has been reported that the lift force of a PL is negative over a scour pit (Yang et al., 2024). The negative lift force was not considered in the calculation of the sagging distance. To refine the prediction method, the lift force should be included in the prediction of sagging. The accuracy of the

above-mentioned method for predicting final scour/sagging depth and the time required is affected the accuracy by the previous empirical formulae for predicting propagation speed of scour pit along the cylinder span (Eq. (29)) and the sagging distance at the centre of the free span (Eq. (33)).

In some 2D studies, the rigid PLs sags into the scour hole with a given sagging distance. Dhamelia et al. (2023a) investigated scour of an elastically mounted vertically vibrating PL that sags into the scour hole with a given sagging distance. They simulated the scour with a constant sagging distance in each case, instead of letting the PL to sag into the scour hole gradually. They found that a PL with a sagging distance of 0.3 times PL diameter have smaller scour depth than smaller sagging distances. In addition, the mean deflection of the PL in the vertical direction is negative, except the case where the vibration reaches its maximum. Lee et al. (2018) and (Lee et al., 2019b) investigated the scour of an 2D elevated PL (positioned some distance above the flat seabed) and found that in addition to the decrease in the scour depth, the time scale of an elevated PL increased with the increase of elevation height. Empirical formulae were developed to predict the scour depth and time scale of elevated PLs.

6. Multiple pipelines

Piggyback PLs and two parallel PLs in tandem are the most common configurations in ocean engineering. A piggyback PL as shown in Fig. 11 (a) comprises a main pipe and a smaller-diameter secondary pipe in a clamp arrangement. Clamping the smaller pipe to the main pipe ensure ensuring the safety of the smaller pipe. If the smaller pipe is attached to the main pipe without a gap between them in a piggyback PL, it is equivalent to a spoiler shown in Fig. 11 (b). Otherwise, the gap between the smaller and main pipes has significant effect on the scour depth (Zhao and Cheng, 2008) because the gap affects the vortex shedding process (Zhao et al., 2007). Two PLs of an equal diameter are sometimes laid together in a tandem arrangement for the convenience of installation and maintenance. The scour below two tandem PLs is affected the distance between them.

Scour could be beneficial for a flexible PL, because it makes the PL sink into the scour hole due to its own weight. Backfill will happens after the PL fully sinks into the scour hole (Sumer and Fredsøe, 2002). Backfill also called self-burial is beneficial for PL stability and significant part of the PL has been observed in prototype engineering projects (Zhu et al., 2019; Yang et al., 2013). Since increased scour depth can contribute self-burial, a spoiler can be attached to the PL to enhance the scour. In this section, piggyback pipelines, two tandem pipelines and a PL with a spoiler are discussed in 6.1, 6.2 and 6.3, respectively.

6.1. Piggyback pipeline

The experimental data by (Salehi and Azimi, 2022) indicated that the maximum and minimum scour depth of a piggyback PL occurs at $\theta_p = 90^\circ$ and 0°, respectively. Zhao and Cheng (2008) investigated scour below a piggyback PL with $d/D = 0.2$ and $\theta_p = 90^\circ$. They found that there is a critical gap defined as G_{cr} between the two pipes below which the two pipes act as a single body hydrodynamically and above which the two pipes have their own individual wakes. For $d/D = 0.2$, G_{cr}/D is between 0.1 and 0.15. The equivalent frontal area of the PL is the maximum and the scour depth reaches its maximum value at $G = G_{cr}$. The mean drag force of the main pipe was found increased significantly compared with the case of a single pipe case. Zhao et al. (2018) conducted experiments of scour below a piggyback PL with $d/D = 0.358$, $\theta_p = 90^\circ$, and $G/D = 0$ to 0.5 with an increment of 0.1. They found the scour depth decreases with the increase of G/D but did not report a critical G_{cr}/D, probably because the increment of $G/D = 0.1$ is insufficiently small to find G_{cr}. Yang et al. (2021) numerically simulated scour below a piggyback PL with $d/D = 0.2$, $G/D = 0$ and θ_p ranging from 0° to 180° with an interval of 15°. The scour depth was found to be the maximum when $\theta_p = 180^\circ$ but smaller than that of the single pile only case when θ_p is between 0° and 30° or between 165° and 180°. Based on the previous studies of flow control (Zhao, 2023), the reason of the reduced scour depth is that putting a small pipe in front or behind the main pipe weakens vortex shedding and consequently weakens the lee wake scour. In the above-mentioned numerical studies, the lift coefficient of the PL is found to point downwards, and this is beneficial for PL self-burial. However, the significant increase in the drag coefficient will increase the horizontal deflection if piggyback PLs are flexible.

SERTA FRAGA et al. (2022) numerically investigated scour of a piggyback PL with two smaller pipes on the upstream and downstream sides of the main pipe, respectively. The two smaller pipes were vertically located below the centre of the main pipe. The deposition of the sediment behind the PL because of the additional smaller pipes causes some blockage of the flow and consequently reduced maximum scour depth.

Yang et al. (2019) conducted experiments of scour below a piggyback PL with $d/D \approx 0.36$ and $\theta_p = 90^\circ$. They found that the scour depth under waves increases with the increase of KC number and decreases with the increase of G/D when G/D is small. If the spacing ratio G/D is greater 0.4, the equilibrium scour depth around the piggyback PL is similar to that in the case of a main pipe only. Huang et al. (2021) numerical simulated scour below a piggyback PL under oscillatory flow with $d/D = 1/3$, $KC = 11$, $G/D = 0.25$ and $\theta_p = 0^\circ, 45^\circ$ and 90°. The scour depth at $\theta_p = 90^\circ$ was found initially greater than the case of a main pipe only, however, backfill occurs in the late stage, making the scour depth reduce and lower than that of a single main pipe. This backfill stage was probably because the oscillatory flow was used instead of free-surface waves, as it was not reported by Yang et al. (2019). Liu et al. (2016) suggested the necessity of using surface wave model instead of oscillatory flow to simulate wave induced scour when the waves were strongly nonlinear.

Hu et al. (2022b) conducted an experimental study of scour below a piggyback PL with $d/D = 1/3$, $\theta_p = 90^\circ$ and $G/D = 0$ to 0.3 under combined waves and current. It was found that the scour depth increases when the gap ratio G/D increases from 0 to 0.1, and it gradually decreases when $G/D > 0.1$. This is in consistent with the conclusion in the steady current case (Zhao and Cheng, 2008). Hu et al. (2022b) conducted experiments of local scour around piggyback PLs with $d/D = 1/3$ and $G/D = 0$ to 0.3. It was found that the upper limit of Eq. (13) by Sumer and Fredsøe (1996) can predict the scour of piggyback PLs well under the test conditions. Hu et al. (2022b) derived the following empirical formula for the time scale of the scour:

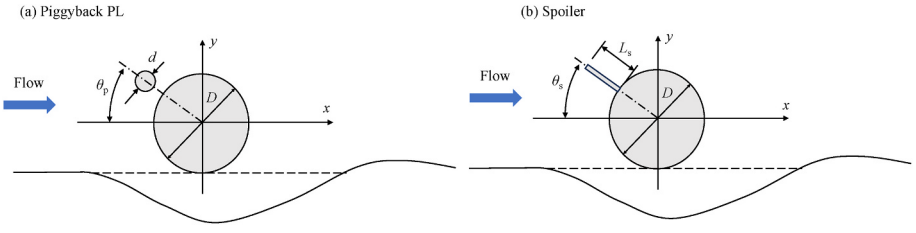

Fig. 11. Sketches of (a) a piggyback PL and (b) a PL with a spoiler.

$$T^* = f(G/D)\theta_{cw}^m \tag{37}$$

where

$$f(G/D) = 0.033 + 0.006 \exp\left[-60.93(G/D - 0.1)^2\right] \tag{38}$$

The format of Eq. (37) follows similar format as Eq. (20) but with varying coefficient $f(G/D)$. The coefficient m is between -1.520 and -1.530 for $G/D = 0$ to 0.3.

6.2. Two pipelines in tandem

Zhao et al. (2015a) simulated scour of two PLs numerically for gap ratios between 0.5 and 5. It was found that the scour depth below the upstream PL is slightly greater than PL, while the scour depth below the downstream PL is much greater than that a single PL. The maximum scour depth of the downstream PL at $G/D = 2.5$ is 50% greater than a single PL. Zhang et al. (2017b) conducted an experimental study and had same conclusion as for $G/D \leq 3$, but found smaller scour depth of the downstream PL than upstream. They found that the scour depths of both PLs are close to that of a single PL if G/D exceeds 6. Hu et al. (2019) used CFD-DEM to simulate scour of two PLs in tandem. They used CFD-DEM to confirm that macroscopic scour development is closely related to the microscopic individual particle behaviour, indicating the advantage of using CFD-DEM. Because the simulations were conducted under live bed condition without sand supply from the upstream of the sand basin, the conclusions are limited to the case that are simulated. Hu et al. (2019) numerically investigated scour of two pipelines in tandem placed in a sand basin without supplied of sand from the upstream. Since sand is not supplied from the upstream the sand basin, the scour depths under live-bed condition are greater than the case where the bed is fully covered by sand.

Li et al. (2020b) investigated scour of two tandem PLs under combined waves and currents using CFD. Their results of currently only case agreed well with Zhao et al. (2015a). It was found that when the flow ratio m = 0 to 0.25, the scour is similar to the purely wave condition and mainly affected by the KC number.

6.3. Enhancement of scour depth using spoilers

When a spoiler is placed vertically on top of a PL, i.e., $\theta_s = 90^\circ$ shown in Fig. 11 (b), the large blockage that it creates forces more of the flow downward beneath the pipe, resulting in an increase of the scour depth (Chiew, 1992). The scour depth increases with the increase of the spoiler length. The upward movement of the stagnation point on the cylinder measured by Yang et al. (2012b) further proves that increased flow going through the gap between the PL and seabed. Yang et al. (2013) numerically approved that the length of the spoiler has significant effects on the scour and the wake of a PL. The numerical study by Zhou et al. (2021) showed that a spoiler with a length-to-diameter ratio $\frac{L_s}{D} = 0.33$ increased the scour depth by 30%.

Different from other studies, Jabari et al. (2021) put the spoiler below the PL at $\theta_s = -90^\circ$ and found that if the spoiler caused increase or reduce the scour depth depends on its length. The maximum reduction of scour depth occurs at a spoiler with $\frac{L_s}{D} = 0.08$, while a spoiler with $\frac{L_s}{D} = 0.2$ increased the scour depth the maximum. In addition to affecting the scour depth, a spoiler underneath a PL reduced the scour length, the size of the scour hole in the horizontal direction. Salehi and Azimi (2022) found that if two PLs are placed in a tandem arrangement, attaching a spoiler on top of the upstream PL can cause more burial of the downstream PL because of the increased scour depth, and the burial depth decreases with the increase of the distance between the two PLs.

Chiew (1993) investigated wave-induced scour of a PL with two spoilers symmetrically put on its top left and top right sides, respectively, for $L_s/D = 0.25$ and 0.5. The maximum lee-wake scour was 4.5 times the maximum scour depth associated with a plain PL. Yang et al. (2012a) tested the effectiveness of a rigid spoiler and a flexible rubble spoiler on the scour enhancement under waves. Both spoilers can increase the scour depth, the rigid spoiler causes sand dunes on the two side of the PL, while the rubble spoiler has little effects on the upstream and downstream bed.

7. Scour protection

Burying a PL should be the most effective way of scour protection, but it is costly and usually implemented in shallow water zone. Several studies have been conducted to protect PLs from scour by covering the seabed surface. The materials used for protecting offshore foundations (Chambel et al., 2024) are also suitable for PL scour protection.

Xie et al. (2019a) proposed geotextile mattress with sloping curtain (GMSC) on the upstream side of a PL for protecting PLs from scour. The GMSC design is shown in Fig. 12 (a), it comprises a mattress made of geotextile tubes filled with sand, a flexible curtain with openings allows sand to pass and a light floating tube raises the curtain into water. The GMSC installed on the upstream side of the PL can effectively reduce the hydraulic gradient across the PL, which is the dominant cause of onset of scour under the pipelines in steady currents. The optimal distance between the GMSC and the PL is 6 times the height of the GMSC. Zhu et al. (2020a) proposed geotextile mattress with floating plate (GMFP), which is similar to the GMSC, only difference is that the sand-pass opening of GMFP is fully opened instead being a row of rectangular shaped openings. They found that the minimum hydraulic gradient under the PL occurs when the $\sin(\alpha) = 0.77$.

Yang et al. (2014) experimentally studied the effectiveness of a horizontal rubber plate below a PL for preventing scour under steady current. A horizontal plate protects the PL from scour by reducing the pressure gradient and seepage flow below the rubber plater, which the key mechanism for scour onset. They derived a formula to predict the minimum plate width that is required to stop scour using theoretical method and validated the formula using experimental data. Karamzadeh et al. (2024) tested the effects of the position of a protective blade below a PL shown in Fig. 12 (b) on the evolution of scour holes. The smallest scour depth occurred when the PL is placed on the downstream edge of the plate with the scour depth reduced by 70%. The largest scour depth occurred when the PL is on the upstream edge of the plate. Hu et al. (2022a) used Ionic Soil Stabilizer (ISS) Solidified Soil to form a plate below a PL for scour prection. The ISS slurry solidifies after they are pours on the sand surface and forms proction layer, and it is cost effective and eco-friendly material. Putting a PL on top of a soft geotexitle mattress could also protect the scour, but its effectiveness has never been assessed. Some other materials that have been used for protecting scour of vertical piles including the tridational riprap stone (Petersen et al., 2015; Wang et al., 2023) microbial-induced carbonate precipitation (MICP) and enzymatic-induced carbonate precipitation (EICP) (Liu et al., 2021a), solidified slurry (OuYang et al., 2022; Wu et al., 2024) also have potential to protect scour of PLs.

8. Pipeline vibration

If the free span of a PL caused by scour is long, the PL will vibrate in both inline and crossflow direction like a beam. The vibration in the crossflow direction should dominate as found in many studies flow-induced vibrations. Flow-induced vibration of slender cylindrical structures is referred to as vortex induced vibration (VIV) as it is mainly driven by vortex shedding. PL vibration is a 3D problem, but nearly all the studies of PL vibration due to scour is investigated using a 2D configuration, where a rigid PL is elastically supported by springs, because the investigation of 3D vibration of PLs is challenging. The studies in sections 8.1 to 8.2 are one-degree-of-freedom (1-DOF) VIV, two-degree-of-freedom (2-DOF) VIV and forced vibrations of an elastically supported rigid PLs on a scoured bed, respectively.

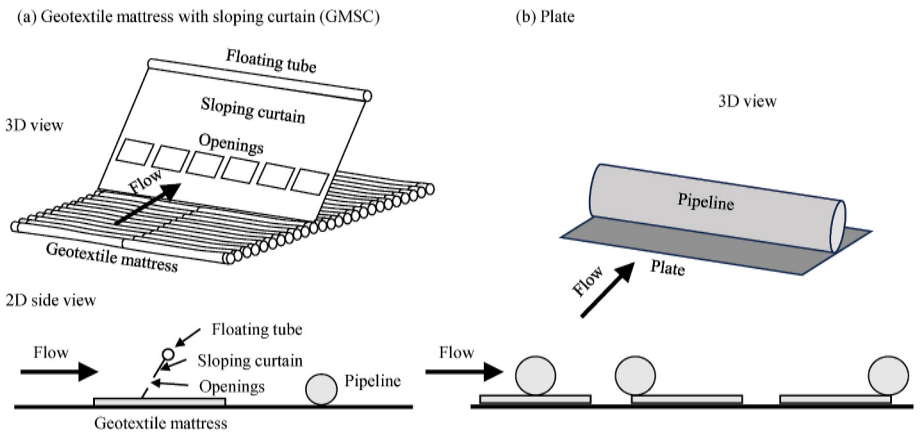

Fig. 12. Scour protection methods. (a) Geotextile mattress with sloping curtain (GMSC) (Xie et al., 2019a). (b) Bottom plate.

8.1. One-degree-of-freedom vibration

Majority of the experimental studies of scour below a free and forced vibrating PL, the PL vibrated with 1-DOF in the vertical direction. In some numerical studies, the PL is allowed to vibrate with 2-DOF in both horizontal and vertical directions. The research outcomes of scour of a vibrating PL in 1-DOF in the vertical direction are summarized below.

(1) Vibration has of two phases. Through experiments of scour of a vibrating PL that was elastically mounted by springs, Gao et al. (2006) found that the scour process has two phases: earlier phase I where the PL does not vibrate and later phase II where the PL vibrates. In the early stage, the PL does not vibrate because there is not vortex shedding. VIV does not exist at the early stage because the vortex shedding does not occur if the gap between the cylinder and the boundary small. Dhamelia et al. (2023a) found two types of transition of vibration during the scour process: Type I where the vibration amplitude decreases and Type II where the vibration amplitude increases, and quantified the timing when these two transitions happen. Type II transition is equivalent to the transition between phases I and II reported by Gao et al. (2006).

(2) Vibration enhances the scour. Increased scour depth of a PL with VIV compared with a fixed PL are reported experimentally (Gao et al., 2006; Sumer et al., 1988b) and numerically (Dhamelia et al., 2023a). Zhang et al. (2019b) found that the scour depth of a VIV PL can be increased to 1.9 times compared with a fixed PL. Liu et al. (2021b) found that in addition to the increasing the scour depth the coupling between VIV and scour increases the maximum vibration amplitude from about 1D to 1.2D. Through experimental visualization Guan et al. (2020) and numerical simulations, it was found that the downward motion of the vibrating PL and interactions between the vortices that sheds from the lower side of the PL are main contributions to the scour depth enhancement. Under waves, the scour depth of a vibrating PL could be increased to twice the scour depth of a fixed PL (Ming-Ming et al., 2022).

(3) Sumer et al. (1988b) reported that VIV does not start until significant scour depth has been developed. The scour before VIV starts is the same as scour below a stationary PL. The starting time of the VIV is essentially the boundary between Phases I and II reported by Gao et al. (2006).

Zhang et al. (2019a) investigated scour of two tandem PLs with VIV for gap ratios of $G/D = 1$ to 4 through numerical simulations. It was found that the scour depth below the downstream PL is smaller than the upstream for all the G/D values. The difference between the scour depths between the two PLs is in consistent with two fixed PLs. For two tandem fixed PLs, Zhang et al. (2017b) reported that the scour depth of the downstream PL is slightly smaller than the upstream. Liang et al. (2023) simulated the interaction between VIV and scour of two tandem PLs and found that there is one merged scour hole if $G/D \leq 2$. When $G/D \geq 3$, vortex shedding occurs from both the upstream and downstream PLs, as a results, there are two scour pits.

8.2. Two-degree-of-freedom vibration

The above discussed studies were focused on the 1-DOF VIV of a PL in the vertical direction. Some research has been done on 2-DOF VIV of a PL in both horizontal and vertical directions. The experimental study by Yang et al. (2013) indicated that the scour depth of a 2-DOF VIV PL has a very small difference from 1-DOF VIV. Zhao and Cheng (2010) conducted numerical simulations of scour of a 2-DOF vibrating pipelines and numerically proved that the increase of the scour depth by the vibration especially in the lock-in regime. The scour depth when there is a synchronization is 25% higher that of a fixed PL. Through flow visualization Zhao and Cheng (2010) found that the vibration enhance the lee wake scour by making the vortices closer to the seabed, which are similar to the observation by Guan et al. (2020). Sumer et al. (1989) investigated 2-DOF VIV of a PL on a scoured bed under waves. It was found that a PL placed in a trench was greatly reduced compared with a PL over a flat bed, and the vibration frequencies in the vertical direction were also decreased. Shi et al. (2022) conducted numerical simulations of scour of a 2-DOF VIV PL under waves and current and found that the water depth has significant effects on the scour under waves when $e/D < 0.4$ and $h/D < 5.2$.

8.3. Forced vibration

Scour of a PL with forced vibration are important as it represents the vibration of the PL that is connected to floating objects, like steel catenary riser (SCR) (Li et al., 2013). The forced vibration of a PL is excited by the motion of the structure that the PL is attached to. Luan et al. (2015) found an increase either in the vibration amplitude or frequency caused increase in the scour depth, and developed an empirical formula for predicting scour depth under a vibrating PL with 1-DOF vibration in the vertical direction:

$$S^* = 1.0 + 1.3123A^{*0.0947} f^{*0.3501} \tag{39}$$

where S^* is the ratio of the scour depth of a vibrating PL to a stationary PL, $A^* = \frac{A}{D}$, A is the vibration amplitude, $f^* = fD/U$ and f is the vibration frequency. Liang et al. (2016) conducted a further numerical study and derived a new formula:

$$S^* = 1.0 + 0.325A^{*0.906} \ln(1.0 + 52.36f^*) \quad (40)$$

Fig. 13 is the comparison between Eqs. (39) and (40) with the numerical results in Liang et al. (2016). Eq. (40) predicts the scour depth equally good as Eq. (39) at large values f^*, and is better than Eq. (39) at small values of f^*.

Guan et al. (2019b) and Tom et al. (2018) conducted experiments to study scour of a forced vertically vibrating PL in quiescent water. Guan et al. (2019b) observed that the scour process is controlled by the falling stage of the PL when the vibration frequency is low and by the rising stage if the vibration frequency is high. Tom et al. (2018) found that the scour profile and flow are symmetric for KC $\leq$ 9, asymmetric for 4$\leq$KC $\leq$ 9 and periodically symmetric for KC $\geq$ 9, where KC is defined as $KC = \frac{2\pi A}{D}$. The switch between symmetric and asymmetric flows are correlated to the switch between vortex shedding patterns reported by Williamson and Roshko (1988).

Zhang et al. (2022c) conducted experiments of scour of a forced vibrating PL in steady current. The scour depth is was found to be dependent on the non-dimensional maximum pipe oscillation velocity by Tom et al. (2018) and on the and non-dimensional pipe acceleration (Tofany et al., 2019). Based on the experimental data Zhang et al. (2022c) derived two formulae for predict equilibrium scour depth and in 2023 (Zhang et al., 2023) they made improvement on the formula and the new formula has been presented in Eq. (25) in section 3 when the equilibrium scour depth was discussed.

9. Prediction of local scour

Traditionally, prediction of local scour has been mainly achieved by numerical models based on Computational Fluid Dynamics (CFD). CFD models can predict evolution of the scour from scour onset until the equilibrium stages. Recently, many Machine Learning (ML) models are also developed to predict the scour depth and speed. In this section, the CFD models and ML models are discussed in section 9.1 and 9.2, respectively.

9.1. Computational Fluid Dynamics (CFD) models

CFD models are increasingly implemented in the recent studies of local scour of subsea structures because of the increasing computer power has made it possible to simulate the scour process. Zhao (2022) classified numerical methods for studying local scour into five catigaries: sediment transport rate models, two-phase models, CFD-DEM (Discrete Element Method) models, equilibrium scour models and depth-averaged models. All these models, except depth-averaged models, have been used in the study of local scour of subsea PLs. The conclusions of numerical models on different aspects of scour have been discussed together with experimental studies in previous sections. This section mainly briefly introduces different types of numerical methods and makes comparisons between them.

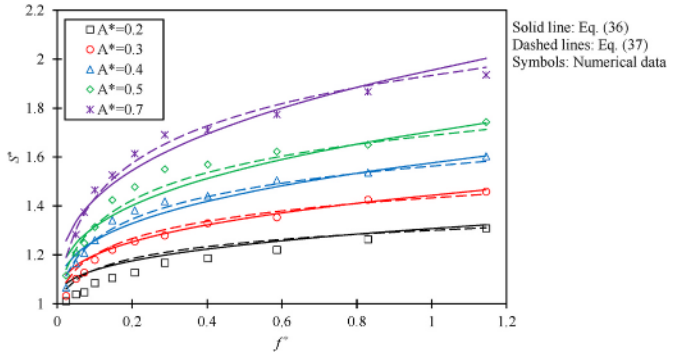

Fig. 13. Comparison between Eqs. (39) and (40) with the numerical results in (Liang et al., 2016).

Sediment transport rate models are the most traditional method, in this model, the motion of the sediment in the flow is quantified by the bed load and suspended load (Sumer and Fredsøe, 2002; Soulsby, 1997), and the evolution of the seabed is predicted by solving the conservation of sediment mass. The time scale for scour simulation is much longer than the flow simulation. To reduce the simulating time, Liang et al. (2005a) developed a time marching scheme where the scour time step is greater than the flow time step.

The two-phase model describing dilute sediment transport (Hsu et al., 2003; Lee and Huang, 2018; Lee, 2019) has the fluid and sediment phases, and each phase have its own mass and momentum conservation equations. Efforts have been made to improve the performance of two-phase models. Lee et al. (2016) proposed a two-phase numerical scheme that overcomes the numerical instability caused by high sediment concentration and allowing the sediment dynamics to be computed both within and outside the sand bed. Lee et al. (2019a) extended the two-phase model to a three-phase (water-air-sediment) model that track both the water-air and sediment-water interfaces. Tofany et al. (2019) and Tofany and Wirahman (2022) implemented the Hybrid Fictitious Domain-Immersed Boundary (HFD-IB) method into the three-phase model by to simulate scour under a vibrating PL and stationary pipelines. The two-phase model has been implemented into open source CFD package OpenFOAM to simulate scour of pipelines (SUBIYANTO & TOFANY, 2024; Tofany et al., 2023).

The DEM initially introduced by Cundall and Strack (1979), has the ability to resolve the granular medium at the particle scale and simulate particle-to-particle interaction. Kloss et al. (2012) developed coupled CFD-DEM model to simulate granular motion in fluid flow, where the motion of an incompressible fluid phase in the presence of a secondary particulate phase is then governed by a modified set of Navier–Stokes equations accounting for the volume fraction occupied by the fluid, and a momentum exchange term. Studies on the application of DEM on local scour around subsea PLs have been mainly focused on the validation of the models. Zhang et al. (2014) used CFD-DEM successfully reproduced the onset of the scour caused by the pressure gradient beneath a partially buried PL and the condition of onset agreed with the experimental measurement. Yang et al. (2018) and Song and Park (2022) used CFD-DEM to investigate the whole scour process from onset, tunnel scour, until lee wake scour. Yang et al. (2018) highlighted that the motion of the thick layer of sand particles during onset scour and tunnel scour stages might not be properly simulated using single-phase models. Hu et al. (2019) investigated scour of two pipelines in tandem using CFD-DEM placed in a sand basin. Since sand is not supplied from the upstream the sand basin, the scour depths under live-bed condition are greater than the case where the bed is fully covered by sand. Ma et al. (2024) implemented porous medium in far field and coarse-grained method in the CFD-DEM model in PL scour study and achieve significant improvement in efficiency without sacrifice accuracy. Large amount of computing time for simulating the motions of great number of particles restricted the application of CFD-DEM in large scale structures. To overcome this drawback of CFD-DEM, Ma and Li (2023) used coarse grains with equivalent hydrodynamic properties of sand particles to increase the computing speed.

Equilibrium scour models are early models that estimate the equilibrium scour depth based the distribution of the shear stress distribution along the seabed (Li and Cheng, 1999, 2000; Lu et al., 2005). They are very efficient to find out the scour profile at equilibrium stage but unable to predict the scour history. This method was rarely used recently with the advanced computing technology.

Since numerical methods do not have restrictions on the model scale, the scaling effects that were involved in all small scale experimental studies of local can be discovered through numerical simulations. Reynolds number or Froude number similarity could not be satisfied in many experiments due to the limitation of the facility. However, numerical simulations of local scour on prototype scales are very rare. My

own eperience of numerical simulations is that, even using the most efficient one-phase sediment transprot model and using the accelerated time marching scheme developed by Liang et al. (2005a), simulations still cost extremely long time to simulate the scour from the onset until equilibrium expecially in 3D simulations. Using 2D numerical methods, Liang et al. (2005b) and Zhao et al. (2011) found that the scour depth decreased with the increase in the Reynolds number.

9.2. Machine learning (ML) models

Many ML models have been developed for predicting scour depth under various conditions including current, waves and combined waves and current. All the ML methods were reported to have better accuracy than simple regression equations. Comparison between different ML models have been the focus in many studies of ML models.

Azamathulla and Ghani (2010) developed a genetic programming (GP) model for predicting socur of pipelines in rivers and found it is more effective than regression equations and artificial neural networks (ANN) modeling in predicting the scour depth. However, Kizilöz et al. (2015) recommended ANN for predicting scour under storm conditions with regular and irregular waves. Azamathulla and Zakaria (2011) further proved that Artificial neural networks (ANN) also perform better than lienar regression method. Azamathulla et al. (2011) developed a linear genetic programming (LGP) mode and an adaptive neuro-fuzzy inference system (ANFIS) model for predicting scour below PLs in current and reported that LGP is better than ANFIS and regrssion equaions Azamathulla and Mohd. Yusoff (2013) further demonstrated that gene-expression programming (GEP) was a good tool tool for predicting scour of river pipelines. Etemad-Shahidi et al. (2011) developed a M5' model tree as a novel soft computing method for predicting the wave-induced scour and reported that this model was more transparent and can provide understandable formulas. Kazeminezhad et al. (2010) used an Artificial Neural Network (ANNs) approach to develop a more accurate model for prediction of wave-induced scour depth around submarine pipelines than empirical methods. Yasa and Etemad-Shahidi (2013) used decision tree and nonlinear regression approaches to develop formulae for estimation of the current induced scour depth and demonstrated that the proposed formulas are more accurate than previous ones in predicting the scour depth in in both live bed and clear water conditions.

Najafzadeh et al. (2014a) utilised back propagation (BP) algorithm in the group method of data handling (GMDH) network for predicting the scour depth below pipelines produced lower error of scour depth prediction than those obtained using the SVM and empirical equations. Najafzadeh and Saberi-Movahed (2019) used the gene-expression programming (GEP) to develop the GMDH network for predicting three-dimensional scour below waves and successfully predicted the longitudinal scour rate. Haghiabi (2017) developed a multivariate adaptive regression splines (MARS) model and found it has high precision for modeling scouring depth under pipelines. Najafzadeh and Sarkamaryan (2018) used data-driven approaches based on gene-expression programming (GEP), evolutionary polynomial regression (EPR) and model tree (MT) to develop explicit equations to estimate local scour depth below pipelines due to currents. Parsaie et al. (2019) reported that the support vector machine (SVM) has higher accuracy than ANN and ANFIS. Sharafati et al. (2020) compared the prediction of wave-induced scour using adaptive neuro-fuzzy inference system (ANFIS) incorporated with particle swarm optimization (ANFIS-PSO), ant colony (ANFIS-ACO), differential evolution (ANFIS-DE) and genetic algorithm (ANFIS-GA).ANFIS-PSO is found to perform better than the other two methods.

Karthikeyan et al. (2020) developed an ANN model by collecting PL accident reports during flooding in the last 35 years to quantify importance of input variables used in predicting critical span length and scour depth based. It was found that factors such as internal fluid pressure, dynamic lateral and vertical soil stiffness, reduced velocity and age of PL have a significant contribution in terms of model weights and help in accurately assessing the PL's vulnerability to failure. Hu et al. (2021) compared the performance of the GABP (Genetic Algorithm based Back Propagation) neural network, RBF (Radial Basis Function) and SVM (Support Vector Machine) and found that the GA-BP model provided the best predictive performance for scour depth exhibiting highest correlation coefficient and lowest Root Mean Square Error. Ehteram et al. (2020) used multilayer perceptron (MLP) models and experimental data of Cheng et al. (2014) to predict the 3D scour speed around a PL due to waves. They tested three models and concluded that the MLP-CBO model performed the best and better than empirical models. Najafzadeh and Oliveto (2021) and Najafzadeh et al. (2022) used four AI models were used to assess the scour propagation rates under current, waves and combined waves and current: Gene-Expression Programming (GEP), Multivariate Adaptive Regression Splines (MARS), M5 Model Tree (M5MT) and Evolutionary Polynomial Regression (EPR), and made detailed discussion on the accuracy and efficiency of these four models. By evaluating the performance of AI models by various statistical measures, Najafzadeh et al. (2022) concluded that their proposed equations performed better than previous reported models in the literature. Najafzadeh et al. (2022) identified that the available data were limited for them to test the AI models. More studies on 3D scour need to be conducted in future.

10. Scaling effects

In experimental studies, the sediment particles are not scaled down following the length scale, resulting different in ratio of D/d_s between the experimental and protype conditions. Most experiments of scour experiments did not follow Reynolds similarity and Froude number similarity. The effects of scaling were investigated in very limited number of studies.

Liang et al. (2005b) and Zhao et al. (2011) proved that small scale experiments overestimated the scour depth compared with the prototype scale using numerical simulations. The numerical study by Zhao et al. (2011) showed that the scour depth decreases linearly with the increase of the model scale. A correlation between the scour depth and model scale is derived based on the numerical simulations:

$$\left(\frac{S_e}{D}\right)_p = \left(\frac{S_e}{D}\right)_m - 0.382\left(D_p - D_m\right) \tag{41}$$

where the subscript 'm' and 'p' stand for the model and prototype scales, respectively. The above equation derived using a model PL with $D_m = 0.05$ m proved that the scour depth increases linearly with the increase of model scale, but it may not be suitable for other generic cases. Moncada and Aguirre-Pe (1999) conducted experiments of scour using various model scales and flow velocities. They concluded that the scour depth increases with the increase of the Froude number, but not sensitive to the Reynolds number. Because all the parameters were varied in their parametric space, the conclusions on the effects of the Reynolds number and the Froude number by Moncada and Aguirre-Pe (1999) were not made by keeping the rest parameters unchanged.

The effects of ratio of pile diameter to sediment particle diameter, and the turbulence scale on the scour around vertical piles have been investigated but not for PLs. Lee and Sturm (2009) found that the ratio of a vertical pile size to the sediment particle size has significant effect on the scour depth. But the effect of D/d_s on the scour of PLs has never been paid attention to. In addition, the turbulence intensity also has significant effect on scour around vertical piles. Ettema et al. (2006) reported that an increase of the pile diameter from 64 mm to 406 mm resulted in a reduction of the scour depth from about $S_0/D = 1.8$ to about $S_0/D = 1.17$ in the experiments by Ettema et al. (2006). Turbulence effects on the scour of PLs have never been considered.

11. Cohesive sediment

Empirical formulae have been developed to predict the erosion rate of the surface of cohesive sediment under flow. Postacchini and Brocchini (2015) derived a formula through theoretical analysis for predicting the wave-induced scour depth under a PL on a cohesive soil, which is a function of KC number and the content of clay. Empirical formulae have been developed to describe the relation between the erosion rate and the shear stress on the sediment surface. The commonly used formula is in the format of:

$$E_s = M(\tau - \tau_c)^b \tag{42}$$

where E_s is the erosion rate and M is a coefficient related to the soil properties. The exponent b in Eq. (42) (42) was recommended to be between 1.5 and 1.7 by Mohr et al. (2016). Parchure and Mehta (1985) found the exponential relationship between the erosion rate and the shear stress:

$$\ln\left(\frac{E_s}{E_f}\right) = M(\tau - \tau_c)^{1/2} \tag{43}$$

where E_f is the erosion rate when $\tau = \tau_c$. The erosion rate is 0 based on Eq. (42) and E_f based on Eq. (43). Van Prooijen and Winterwerp (2010) used stochastic analysis to derive a formula for erosion rate:

$$\frac{E}{M\tau_c} = \begin{cases} 0, \frac{\tau_b}{\tau_c} < 0.52 \\ a_1\left(\frac{\tau_b}{\tau_c}\right)^3 + a_2\left(\frac{\tau_b}{\tau_c}\right)^2 + a_1\left(\frac{\tau_b}{\tau_c}\right) + a_4, 0.52 \le \frac{\tau_b}{\tau_c} \le 1.7 \\ \frac{\tau_b}{\tau_c} - 1, \frac{\tau_b}{\tau_c} > 1.7 \end{cases} \tag{44}$$

where $a_1 = -0.144$, $a_2 = 0.904$, $a_3 = -0.828$ and $a_4 = -0.204$. When $\frac{\tau_b}{\tau_c} > 1.7$ Eq. (44) is the same as Eq. (42) with $b = 1$. The erosion rate is not zero when $\tau_b = \tau_c$ as per Eq. (41).

In the experiments of scour of PLs laid on cohesive sediment, Mohr et al. (2016) found that there was no deposited sediment observed downstream of the PL, indicating that the scour occurring predominantly through entrainment of sediment from beneath the PL. Based on this observation, the scour evolution of scour profile with cohesive sediment can be predicted using combination of CFD and the above-mentioned formulae for predicting erosion rate.

Zang et al. (2024) developed a numerical model for simulating scour of a PL on top of cohesive sediment where the flow is simulated by CFD and the scour is predicted by Eq. (42) and Eq. (44). They found that predicted erosion depth using Eq. (42) with $b = 1.5$ in the wake of the PL is higher than that from $b = 1$ and Eq. (44), mainly because it predicts higher erosion rate at high shear stress due to the vortex shedding. They emphasized that using a erosion rate formula that correctly represent the soil is important. The numerical method predicted a regular and smooth scour profile agreed well with the experimental data of artificial sand-silt mixture but not well with the natural sand-silt mixture. The measured scour profiles of natural sand-silt mixture were much more irregular. Zhu et al. (2019) hypothesed that the randomness of the scour is caused by randomness of turbulences. The numerical models based on RANS does not have very irregular scour profiles because the randomness of the turbulence was filtered out.

Under same flow velocity scour of cohesive sediment is weaker than loose, invicid sand. Zang et al. (2021) experimentally investigated the interaction between scour and VIV of a PL on a silty seabed surface. The scour depth of the silty seabed is found to be about 1/3 smaller than that of the loose inviscid sand surface. The onset velocity for the vibration to occur was found to be dependent on the scour depth.

12. Conclusions and recommendations

12.1. Conclusions

This paper presented a comprehensive review of the research on scour below subsea pipelines. The review covering a variety of topics including onset of scour, scour depth and time scale, 3D scour, sagging, multiple PLs, scour enhancement, scour protection, PL vibration and scaling effects. This paper can enable the readers to have a good understanding of the outcomes of the previous studies and identify new research objectives in this field.

1. Nearly all the above-mentioned topics except 3D scour have been conducted under simplified 2D configurations because of the availably of the 2D experimental facilities and the achievability of 2D numerical simulations. Empirical formulae derived for predicting the equilibrium scour depth, the time scale, the scour depth of sagging and vibrating PLs are useful for predicting scour in engineering projects.
2. 3D studies have been focused on quantifying the propagation speed of scour hole along the spanwise direction under current and waves, and empirical formulae have been developed to predict the speed. The investigation of the 3D scour speed was measured using rigid PL models.
3. The 3D sagging problem was simplified to 2D problem of the sagging of the mid-section of the suspended free span, with the sagging distance calculated by empirical method in many studies. The vibration of a flexible PL is simplified as the vibration of a 2D PL supported by springs. Considering that the degree of curvature of a real PL is very small, the above simplification reasonably represents the scour at the mid-section.
4. More numerical studies were conducted than experimental studies since 2000. However, numerical studies were mostly conducted in small scale PLs same as those in the experimental condition. Majority of numerical simulations used 2D models to enable the scour process to be simulated with affordable computing time. Solving the RANS equations is the most common method for simulating the scour and flow in single phase models. In the two-phase models, sediment phase and flow phase have their own continuity equations and momentum equations.
5. Very limited number of studies have been conducted on the scaling effects and they were mainly through numerical simulations. In addition to the conclusion that the scour depth is found to decrease linearly with the increase of the model scale, not empirical formulae that consider the combination effects of Re, Fr and D/d_s have been proposed.
6. ML models are proven be more accuracy than simple empirical formulae. It has been identified that the available experimental/field data for developing accurate ML models are limited, especially on 3D scour. Mode data is required to further improve ML models.

12.2. Recommendations on future studies

After reviewing the studies of scour below PLs, the following aspects of scour which are important but not fully understood are identified. They should be the objectives of future studies.

1. The effects of scaling were not fully understood and should be further investigated. The effects of the PL to sediment particle diameter ratio, the turbulence scale have been proven in scour of pile structures but have never studied for PL scour. It was found that the scour depth decreases with the increase of model scale, but model scale effects have not been properly quantified.
2. Scour of PLs were mainly investigated use small scale PL models in both experimental and numerical methods where the Reynolds number is in the order of 10^4. It has been proven that the lee wake

scour dominates the late stage of scour process. Vortex shedding changes significantly as the Reynolds number increases from the sub-critical regime ($300 < Re < 3 \times 10^5$) to critical regime and super critical regime ($3.5 \times 10^5 < Re < 1.5 \times 10^6$), where the wake becomes narrow with smaller vortices (Rodríguez et al., 2015; Sumer and Fredsøe, 2006). The Reynolds numbers of prototype PLs are mostly in the order of 10^6. It is necessary to conduct large scale experiments to identify how increasing Re to the super critical regime will affect the lee wake scour.

3. While focus has been placed on the evaluation of scour depth under various conditions, PL self-burial has never been properly investigated. The sagging of a PL until it reaches the bottom of scour hole has been studied experimentally and numerically and the ultimate sagging distance has been quantified. After sagging, further investigation should be conducted to understand how a PL will be self-buried and quantify the self-burial depth.
4. The studies of 3D scour are much fewer than 2D scour. Different studies have contradictory conclusions when 3D scour is investigated (see section 4). It is not quite sure if the contradiction is because the test conditions were different (live-bed or clear-water scour) or because the water flume (PL length) is not sufficiently wide in the studies. Increasing 3D studies need to be conducted to fully understand the scour process and improve the prediction accuracy of scour propagation speed.
5. Scour of PLs over cohesive sediment has been studied much less than loose, inviscid sand. The former is much more challenging than the latter because the much more sediment properties affect the scour and types of sediments found in ocean are very diverse. Since cohesive sediment is very common in the ocean, it is necessary to do more research to improve the understanding of scour of cohesive sediment.
6. Nearly all numerical studies have been conducted using small scale same as in experimental conditions. It should be encouraged to validate numerical models in large scale protype conditions and implement them to overcome the weakness of experiments on scaling.
7. Limited number studies have been conducted on scour protection, and some proposed protection methods appear to be complex although effective. It is recommended more research need to be focus on cost effective protection methods.

Declaration of competing interest

The authors declare that they have no known competing financial interests or personal relationships that could have appeared to influence the work reported in this paper.

Appendix. List of key research outcomes of studies of pipeline scour

In this appendix, the key findings of previous studies are summarized very concisely in Table A1. The topic of each study can be seen through key words.

Table A1
List of key findings of articles in local scour below pipelines sorted by years.

References	Key words	Key findings
Fredsøe et al. (1988)	3D scour	A simple equation was developed to calculate the span length of the 3D scour hole.
Sumer et al. (1988b)	VIV	Increased scour depth by VIV and dominance of vortex shedding in scour process.
Sumer et al. (1988a)	Scour mechanisms	Lee wake scour caused by vortex shedding governs the scour downstream a PL.
Sumer et al. (1989)	VIV, waves	A PL in scour trench has less vibration than a PL fully exposed to waves.
Sumer and Fredsøe (1990)	Waves	KC number is the main parameter that governs the equilibrium scour depth.
Chiew (1991)	Maximum scour depth prediction	An iterative method for estimating maximum scour depth at submarine PLs.
Fredsøe et al. (1992)	Time scale	The non-dimensional time scale is proportional to the −5/3 power of the Shields parameter.
Chiew (1992, 1993)	Spoilers	A spoiler attached to a PL increases the rate and extent of erosion around a PL under currents and waves.
Moncada and Aguirre-Pe (1999)	Scaling effects	The Reynolds number of the pipe exerts a negligible influence on the scour. The Froude number was found to be an important parameter in the definition of the scour process.
Çevik and Yüksel (1999)	Waves	A new equation for predicting the scour depth.
Li and Cheng (1999)	Scour model for equilibrium scour profile	A numerical model, based on potential-flow theory for simulating the equilibrium scour hole.
Brørs (1999)	RANS scour model	A RANS model was developed.
Li and Cheng (2000)	2D scour	A numerical model for predicting equilibrium scour profile.
Sumer et al. (2001)	Scour onset, self-burial	The mechanisms of onset of scour and self-burial were found.
Dupuis and Chopard (2002)	LBM method	Scour model based on lattice Boltzmann method (LBM) was developed.
VIJAYA KUMAR et al. (2002)	Sagging, cohesive sand	Wave force reduces when the pipeline sags into the scour hole.
Cheng and Li (2003)	Sagging	The ultimate scour depth depends on the sagging speed.
Liang et al. (2005a)	One-phase model	A new time marching scheme and a sand slide scheme to increase simulation speed.
Lu et al. (2005)	Equilibrium scour	A numerical model for predicting the equilibrium profile of local scour around submarine pipeline.
Liang and Cheng (2005)	Waves	Using period averaged sediment transport rate significantly reduces the computational costs and is of acceptable accuracy.
Liang et al. (2005b) and Zhao et al. (2011)	Scaling effects	Scour depths for prototype pipelines are smaller than those for model pipelines.
Gao et al. (2006)	VIV	Scour of a vibrating pipeline has two phases: Phase I where scour beneath pipe without VIV and Phase II where pipeline vibrates.
Zhao and Fernando (2007)	Two-phase model	A two-phase model considering fluid-particle and particle-particle interactions.
Zhao and Cheng (2008)	Piggyback PL	The flow and the scour profiles are influenced significantly by the gap between the two pipes.
Dey and Singh (2008)	Non-uniform sand	An armor layer reduces scour.
Myrhaug et al. (2008)	Waves	The scour depth formula for regular waves can be applied for random waves.
Mousavi et al. (2009)	Waves	When the embedment depth a PL exceeds a specified depth, no scour occurs underneath it.
Cheng et al. (2009)	3D scour	A formula for predicting scour propagation velocity along a PL.
Zang et al. (2009)	Scour onset	Empirical formulae for onset conditions in currents and waves.
Myrhaug et al. (2009)	Waves	The second-order wave asymmetry increases the scour depth below a PL.
Alam and Cheng (2010a)	2D Lattice Boltzmann Model	A 2D LBM model was developed and validated.

(continued on next page)

Table A1 (*continued*)

References	Key words	Key findings
Alam and Cheng (2010b)	LBM model	The existence of a spiral vortex in the proximity of the span shoulder is confirmed.
Zhao and Cheng (2010)	VIV	A 2-DOF vibrating PL has deeper scour depth than 1-DOF.
Azamathulla and Ghani (2010)	Genetic programming (GP)	GP is more effective than regression equations and artificial neural networks.
Azamathulla et al. (2011)	Linear GP model	LGP model has lower RMSE error and higher accuracy than other methods.
Azamathulla and Zakaria (2011)	Artificial neural networks (ANN)	ANN is more effective than regression equations in predicting the scour depth.
Etemad-Shahidi et al. (2011)	Waves	Machine learning based formulae were developed to predict clear and live-bed scour in waves.
Kim et al. (2011)	Waves	Scour was predominantly affected by the KC number.
Kazeminezhad and Yeganeh-Bakhtiary (2011)	Two-phase model	Eulerian two-phase mode was used to simulate tunnel scour stage.
Zanganeh et al. (2012)	Two-phase model	Smoothed Particle Hydrodynamics (SPH) model was developed.
Zhao et al. (2012a)	Scour monitoring	A three-index estimator for scour monitoring under submarine PLs.
Yang et al. (2012b)	Spoilers	Formulas were developed to predict scour.
Yang et al. (2012a)	Spoilers	Rubber plates increases scour depth like a rigid spoiler but have little effect on the upstream and downstream bed.
HOSSEIN KAZEMINEZHAD et al. (2012)	Two-phase model	Tremendous sediment transport takes place during the tunnel scour stage under high turbulence intensity.
Zhao et al. (2012b)	Scour monitoring	A scour monitoring system of subsea pipeline was proposed.
Wu and Chiew (2012)	3D scour	The propagation of the scour hole in the transverse direction of flow is divided into a rapid and a slack phase of development.
Yang et al. (2013)	2DOF-VIV	There is not much difference of the scour profiles around the 1-DOF and 2-DOF vibrating pipes.
Wu and Chiew (2013)	3D scour	The concentrated and strong flow and the transverse flow affects the scour.
Yeganeh-Bakhtiary et al. (2013)	Two-phase model	The numerical model provides a useful approach to improve mechanistic understanding of hydrodynamic and sediment transport in live-bed scour beneath a marine pipeline.
Zhao et al. (2013)	Scour monitoring	A scour monitoring system for subsea pipeline is proposed.
Zhu et al. (2013)	Spoilers	Spoiler length and the PL level affect the scour.
Kílöz et al. (2013)	Waves	Multiple regression analysis is used to develop models to predict the scour depth.
Azamathulla and Mohd. Yusoff (2013)	GEP programming	This study presents gene-expression programming (GEP) as an alternative soft computing tool for the prediction of scour below underwater pipeline across river.
Yang et al. (2014)	Protection	A rubber plate place underneath the pipe can significantly reduce the pressure difference between upstream and downstream of a PL.
Najafzadeh et al. (2014a)	GMDH network	Using of back propagation produced lower error of scour depth prediction than using the support vector machines (SVM) and empirical equations.
Najafzadeh et al. (2014b)	GMDH network	The GMDH network predicted scour depth more accurately than other models.
Fuhrman et al. (2014)	Waves	A numerical model developed for scour and back fill.
Luo et al. (2014)	3D scour, sagging	A simple calculation model was proposed
Azamathulla et al. (2014)	Skewed pipeline	The study investigated four different pipeline orientations installed from the side wall of the channel.
Zhao et al. (2014)	Scour monitoring	A two-layer BP neural network was employed to process the monitoring data and achieved media recognition.
Zhang et al. (2014)	CFD-DEM	CFD–DEM is a promising numerical tool for future investigations of the mechanism.
Cheng et al. (2014)	3D scour, waves	A formula for predicting scour propagation velocity along a PL.
Kizilöz et al. (2015)	ANN	Artificial Neural Network (ANN) models for predicting the scour depth beneath submarine pipelines for different storm conditions.
Wu and Chiew (2015)	3D scour	A high differential pressure significantly enhances pipeline scour hole development in the spanwise direction.
Zhao et al. (2015b)	Scour monitoring	A novel scour automatic detection scheme was proposed to realize automatic diagnosis of pipeline scour.
Luan et al. (2015)	Forced vibration	Generic relationships are established between the non-dimensional scour depth and the non-dimensional vibrating amplitude and frequency.
Cao et al. (2015)	ANSYS Fluent	ANSYS Fluent was used to predict scour in South China sea.
Postacchini and Brocchini (2015)	Cohesive sand	A new formula when the seabed is characterized by a relatively small clay content.
Zhao et al. (2015a)	Two PLs	The maximum scour depth below the downstream of a PL occurs when the gap-to-diameter ratio is 2.5.
Liu et al. (2016)	Waves	It is necessary to utilize the free surface wave model rather than the simplified oscillatory flow model for strongly nonlinear waves.
Larsen et al. (2016)	Wave-current	A new generalized expression for the scour time scale in combined wave-current.
Zhang et al. (2016a)	Scour onset	The onset of tunnel scour may occur at a lower velocity if the upstream sediment supply is restricted.
Zhang and Shi (2016)	ANSYS Fluent	ANSYS Fluent can provide good prediction of scour.
Zhang et al. (2016b)	varying flow	The effective time scales of the scour and backfill were quantified and algorithms to predict the scour process in changing flow conditions were derived.
Mohr et al. (2016)	Cohesive sediment	Two new empirical formulas for predicting the time scale of the scour process beneath subsea pipelines.
Lee et al. (2016)	Multi-phase model	The model predicted the scour rate well but was unable to capture vortex shedding accurately.
Haghiabi (2017)	Multivariate adaptive regression splines (MARS)	The accuracy of MARS model is slightly lower than that of the MLP multilayer perceptron (MLP) neural network, but better than empirical formulae.
Fan et al. (2017)	Water jump effect	The bed shear stress and scour hole depth computed with the rigid lid approximation were underestimated compared than the free-surface model.
Zhang et al. (2017a)	Scour depth and time scale	A new method of predicting the equilibrium scour depth and time scale for waves and current.
Zhang et al. (2017b)	Two PLs	The maximum scour depth below the downstream PLis deeper when G/D < 3.
Tom et al. (2018)	Force vibration	The scour profile and flow are symmetric for $KC \leq 9$, asymmetric for $4 \leq KC \leq 9$ and periodically symmetric for $KC \geq 9$.
Sharafati et al. (2018)	Stochastic method	The developed stochastic methods were more efficient compared with the deterministic models in prediction of wave-induced pipeline scour depth with consideration of uncertainty.
Ajdehak et al. (2018)	Sagging	A formula for predicting the time history of scour depth prior to touchdown.
Zhao et al. (2018)	Piggyback PL	An empirical to predict the maximum scour depth.
Lee et al. (2018) Lee et al. (2019b)	Elevated PL	Empirical formulae for scour depth and time scale considering PL elevation.
Yang et al. (2018)	CFD-DEM	During the tunnel erosion stage, the particle motion and particle–particle interactive forces are particularly intense.
Xie et al. (2019a)	Protection	A geotextile mattress with sloping curtain (GMSC) was introduced to protect underwater PL.

(*continued on next page*)

Table A1 (*continued*)

References	Key words	Key findings
Mathieu et al. (2019)	Two-phase model	The turbulence model has a significant influence on the bed morphology.
Tofany et al. (2019)	Two-phase model	The maximum pipe acceleration has a dominant effect on the underlying physics that induce scour.
Xie et al. (2019b)	3D scour	visualization tests on the three-dimensional scour process beneath to found scour mechanisms
Zhang et al. (2019b)	VIV	The effects of initial gap-to-diameter ratio, reduced velocity, and pipeline diameter on the local scour and pipeline vibration were investigated
Zang et al. (2019)	Wave-current	Empirical and theoretical approaches for scour depth and scour time scale.
Yang et al. (2019)	Piggyback PL	Both the scour depth and width around piggyback PL is much larger than those around single pipe.
Zhu et al. (2019)	Spoilers	PLs with spoilers gradually self-buried into the seabed
Hu et al. (2019)	Two PL,	The effect of the gap between the two PLs were quantified.
Bastian et al. (2019)	Self-burial, waves	A new and generalized expression for estimating the wave-induced backfilling.
Ahmad et al. (2019)	Wave-current	The correlation between oscillatory velocity and scour.
Zhang et al. (2019c)	Waves	An empirical for the scour in the Yellow River delta.
Guan et al. (2019b)	Forced vibration	The rolls of PL falling and rising in scour development are different.
Zhang et al. (2019a)	Two PLs, VIV	Vibration enhances the scour. The scour depth under the upstream PL is deeper.
Parsaie et al. (2019)	Support Vector Machine (SVM)	The accuracy of SVM is a bit better than artificial neural network (ANN) and Adaptive Neuro fuzzy Inference Systems (ANFIS).
Guan et al. (2019a)	Flow visualization	An experimental method for visualizing flow and scour.
Zhu et al. (2020a)	Protection	A geotextile mattress with floating plate (GMFP) protect the scour by reducing the hydraulic gradient below a PL.
Sharafati et al. (2020)	adaptive neuro-fuzzy inference system (ANFIS), wave	Adaptive neuro-fuzzy inference system (ANFIS) incorporated with particle swarm optimization (ANFIS-PSO) performs better than other methods.
Karthikeyan et al. (2020)	ANN	The internal fluid pressure, dynamic lateral and vertical soil stiffness, reduced velocity and age of pipeline have a significant contribution in terms of model weights and help in accurately assessing the pipeline's vulnerability to failure
Guan et al. (2020)	VIV	The roles of vortices on scour development were discussed.
Ehteram et al. (2020)	3D scour	The MLP-CBO model performed better in comparison to the MLP-PSO, MLP-WA, regression, and empirical models.
Cheng et al. (2020)	Waves	Normalized scour depth by the vortex street size can be simply taken to be a constant for both wave-alone and wave-plus-current conditions.
Zhu et al. (2020b)	Scour onset, Wave scour	The onset of scour in waves does not occur until the average seepage hydraulic gradient exceeded the critical value several times.
Li et al. (2020b)	Waves-current, two PLs	The effects of the pipeline-pipeline distance and wave-to-current velocity ratio are discussed in detail.
Yan et al. (2020)	New numerical method	A mixed moving-mesh and fixed-grid method is developed.
Li et al. (2020a)	upward seepage	For the clear-water case with a large upward hydraulic gradient the equilibrium scour depth slightly decreases.
Vosoughi and Hajikandi (2020)	Waves	Under clear-water condition, the scour depth will be reduced compared with live-bed scour.
Hu et al. (2021)	Machine learning	Froude number (Fr) is the most effective parameter for predicting the scouring depth below the pipeline.
Li et al. (2021a)	Liquification, waves	With increasing scour depths, the maximum liquefaction depth beneath the pipeline simultaneously decreases.
Liu (2021)	Waves	On a slope, the deposition was found on the downslope side and erosion was found on the upslope side of the PL.
Zang et al. (2021)	Cohesive sediment	An empirical formula is proposed.
Myrhaug and Ong (2021)	Waves	A practical stochastic method is derived for the time scale of equilibrium pipeline scour.
Dogan and Arisoy (2021)	Waves	Prediction method for scour along the spanwise direction was developed.
Zhao et al. (2021)	Solitary wave +current	Currently plays dominant role when its non-dimensional velocity is greater than 0.2.
Damroudi et al. (2021)	Spoiler, piggyback PL	The effects of a spoiler and a piggyback PL on the scour process are similar to each other.
Huang et al. (2021)	Waves, piggyback PL	Scour depth is the maximum when the smaller pipe is on the top of the large one.
Yang et al. (2021)	Piggyback PL	Scour depth is the maximum when the smaller pipe is on the top of the large one.
Zhou et al. (2021)	Spoilers	Larger spoiler length leads to a deeper scour depth, and an empirical equation was proposed.
Zhang et al. (2021)	Tidal current	The scour depth in tidal current was 80% that under a steady current.
Sui et al. (2021)	3D scour	New rational formulation for predicting both the primary and secondary span shoulder migration velocities in the live-bed regime.
Liu et al. (2021b)	VIV	the maximum vibration amplitude of the pipeline can reach about 1.2D.
Najafzadeh and Oliveto (2022)	Machine learning model	Machine learning (ML) models are applied for the prediction of the scouring rate in current.
Najafzadeh et al. (2022)	3D scour	Evaluation of 3D scour using AI models.
Hu et al. (2022a)	Protection	Ionic Soil Stabilizer (ISS) is tested and proved reliable and economic material for scour protection.
Liang et al. (2022)	3D scour	ANSYS Fluent solver was proved to be able to solve 3D scour problem.
Hu et al. (2022b)	Piggyback PL	The S_e below the piggyback pipeline increases when G/D increases from 0 to 0.1, and it gradually decreases when G/D $>$ 0.1
Salehi and Azimi (2022)	Piggyback PL	The maximum and minimum scour depth of a piggyback PL occurs at $\theta_p = 90^\circ$ and 0°, respectively.
Tofany and Wirahman (2022)	Scour onset, Two-phase	The onset is triggered by the piping mechanism induced by the upstream–downstream pressure gradient beneath the pipe.
SERTA FRAGA et al. (2022)	Piggyback PL	The effects of the angular position of the piggyback pipe and its gap from the main pipeline.
Zhu et al. (2022)	Waves	The scour development was observed with a miniature camera sealed in a transparent pipeline.
Shi et al. (2022)	VIV, waves-currents	The strong vibration affects the scour process near the pipeline.
Ming-Ming et al. (2022)	Waves, VIV	Vibration deepens the scour and widens the scour extent.
Zhang et al. (2022c)	Forced vibration	Empirical formulas for the prediction of the maximum scour depth and width are proposed.
Tsai et al. (2022)	Two-phase model, backfill	The model is able to reproduce the whole process of scour.
Song and Park (2022)	CFD-DEM	Three scour development process, such as onset of scour, tunnel erosion, and lee-wake erosion, were studied and discussed.
Zhang et al. (2022b)	Waves	A simple formula for predicting the scour depth beneath pipelines under waves in sandy seabeds is suggested.
Hu et al. (2023)	Influence factors	The process of pipeline scour can be divided into clearance scour, wake scour and equilibrium scour.
Farooq et al. (2023)	Scour monitoring	The application of active thermometry techniques for bridge and PL scour monitoring.
Ma and Li (2023)	CFD-DEM	Coarser grain with equivalent hydrodynamic properties can reduce the computation time without bring noticeable error to the results.

(*continued on next page*)

Table A1 (*continued*)

References	Key words	Key findings
Dhamelia et al. (2023a)	VIV	Scour rate and the vibration amplitude change suddenly at a critical time for reduced velocities inside the lock-in regime.
Dhamelia et al. (2025)	VIV	Scour below a pipeline with 2-DOF VIV was compared with 1-DOF VIV.
Zhang et al. (2023)	Forced vibration	A new empirical formula for predicting the scour history.
Liang et al. (2023)	Two PLs, VIV	The gap between the two PLs significantly affects the depth and profile of the scour pits.
Dhamelia et al. (2023b)	Wave-current	The effects of the combined flow ratio of the steady to oscillatory flow velocities on the scour are quantified.
Liu et al. (2023)	PL roughness	The RMS value of the lift coefficient, the scour depth and the scour width decrease with increasing roughness and then change slowly.
Zang et al. (2024)	Cohesive sediment	It is recommended to utilize the erosion rate formula that is calibrated to the specific sediment type based on experimental data for precise numerical prediction of scour process.
Zhai and Jeng (2024)	Waves	The influence of seepage and soil response on the modified Shields number, repose angle and prediction of the local scour depth and profile are examined.
Ma et al. (2024)	CFD-DEM model	CFD-DEM can give an insight into scour mechanics from the aspects including seepage and flow-particle interaction
Karamzadeh et al. (2024)	Protection	The impact of the protective blade on the geometric features was examined.

References

Ahmad, N., Bihs, H., Myrhaug, D., Kamath, A., Arntsen, Ø.A., 2019. Numerical modelling of pipeline scour under the combined action of waves and current with free-surface capturing. Coast Eng. 148, 19–35.

Ajdehak, E., Zhao, M., Cheng, L., Draper, S., 2018. Numerical investigation of local scour beneath a sagging subsea pipeline in steady currents. Coast Eng. 136, 106–118.

Alam, M.S., Cheng, L., 2010a. A 2-D model to predict time development of scour below pipelines with spoiler. AIP Conf. Proc. 993–998.

Alam, M.S., Cheng, L., 2010b. A parallel three-dimensional scour model to predict flow and scour below a submarine pipeline. Cent. Eur. J. Phys. 8, 604–619.

Azamathulla, H., Yusoff, M.A.M., Hasan, Z.A., 2014. Scour below submerged skewed pipeline. J. Hydrol. 509, 615–620.

Azamathulla, H.M., Ghani, A.A., 2010. Genetic programming to predict river pipeline scour. J. Pipeline Syst. Eng. Pract. 1, 127–132.

Azamathulla, H.M., Guven, A., Demir, Y.K., 2011. Linear genetic programming to scour below submerged pipeline. Ocean Eng. 38, 995–1000.

Azamathulla, H.M., Mohd Yusoff, M.A., 2013. Soft computing for prediction of river pipeline scour depth. Neural Comput. Appl. 23, 2465–2469.

Azamathulla, H.M., Zakaria, N.A., 2011. Prediction of scour below submerged pipeline crossing a river using ANN. Water Sci. Technol. 63, 2225–2230.

Bastian, K., Carstensen, S., Sui, T., Fuhrman, D.R., 2019. Generalized time scale for wave-induced backfilling beneath submarine pipelines. Coast Eng. 143, 113–122.

Bijker, E.W., Leeuwestein, W., 1984. Interaction between pipelines and the seabed under the influence of waves and currents. Seabed Mechanics. Edited Proc. IUTAM and IUGG Symposium, pp. 235–242. Newcastle, 1983.

Briaud, J.L., Ting, F.C.K., Chen, H.C., Gudavalli, R., Perugu, S., Wei, G., 1999. SRICOS: prediction of scour rate in cohesive soils at bridge piers. J. Geotech. Geoenviron. Eng. 125, 237–246.

Brørs, B., 1999. Numerical modeling of flow and scour at pipelines. J. Hydraul. Eng. 125, 511–522.

Cao, Y., Bai, Y., Wang, J., Liao, S., Xu, D., 2015. Prediction of scour depth around offshore pipelines in the South China Sea. J. Mar. Sci. Appl. 14, 83–92.

Çevik, E., Yüksel, Y., 1999. Scour under submarine pipelines in waves in shoaling conditions. J. Waterw. Port, Coast. Ocean Eng. 125, 9–19.

Chambel, J., Fazeres-Ferradosa, T., Miranda, F., Bento, A.M., Taveira-Pinto, F., Lomonaco, P., 2024. A comprehensive review on scour and scour protections for complex bottom-fixed offshore and marine renewable energy foundations. Ocean Eng. 304, 117829.

Chen, C., Zhang, J., 2009. A review on scour modeling below pipelines. Pipelines 2009: Infrastructure's Hidden Assets - Proceedings of the Pipelines 2009 Conference, pp. 1019–1028.

Cheng, L., Li, F., 2003. Modelling of local scour below a sagging pipeline. Coast Eng. J. 45, 189–210.

Cheng, L., Yeow, K., Zang, Z., Li, F., 2014. 3D scour below pipelines under waves and combined waves and currents. Coast Eng. 83, 137–149.

Cheng, L., Yeow, K., Zhang, Z., Teng, B., 2009. Three-dimensional scour below offshore pipelines in steady currents. Coast Eng. 56, 577–590.

Cheng, L., Zhao, M., 2010. Numerical Model for Three-Dimensional Scour below a Pipeline in Steady Currents, pp. 482–490.

Cheng, N.S., Chiew, Y.M., Chen, X., 2016. Scaling analysis of pier-scouring processes. J. Eng. Mech. 142, 1–6.

Cheng, N.S., Wei, M., Xu, P., Mao, R., 2020. Length scale for evaluating wave-induced pipeline scour. Ocean Eng. 218, 108153.

Chiew, Y.M., 1990. Mechanics of local scour around submarine pipe. J. Hydraul. Eng. 116, 515–529.

Chiew, Y.M., 1991. Prediction of maximum scour depth at submarine pipelines. J. Hydraul. Eng. 117, 452–466.

Chiew, Y.M., 1992. Effect of spoilers on scour at submarine pipelines. J. Hydraul. Eng. 118, 1311–1317.

Chiew, Y.M., 1993. Effect of spoilers on wave-induced scour at submarine pipelines. J. Waterw. Port, Coast. Ocean Eng. 119, 417–428.

Cundall, P.A., Strack, O.D.L., 1979. A discrete numerical model for granular assemblies. Geotechnique 29, 47–65.

Damroudi, M., Esmaili, K., Rajaei, S.H., 2021. Effect of pipeline external geometry on local scour and self-burial time scales in current. J. Appl. Fluid Mech. 14, 103–115.

Dey, S., Singh, N.P., 2008. Clear-water scour below underwater pipelines under steady flow. J. Hydraul. Eng. 134, 588–600.

Dhamelia, V., Zhao, M., Hu, P., 2023a. Numerical investigation of local scour around a vertically vibrating subsea pipeline under steady flow. Ocean Eng. 285, 115437.

Dhamelia, V., Zhao, M., Hu, P., Mia, M.R., 2023b. Numerical investigation of the local scour around subsea pipelines in combined steady and oscillatory flow. Int. J. Offshore Polar Eng. 33, 47–53.

Dhamelia, V., Zhao, M., Hu, P., Palmer, H., 2025. Numerical investigation of local scour around a 2-degree of freedom vibrating subsea pipeline in steady flow under sagging condition. Ocean Eng. 315, 119890.

Dogan, M., Arisoy, Y., 2021. The propagation of wave scour along the spanwise direction of submarine pipelines in case of clear-water regime. Coast Eng. 168, 103958.

Dogan, M., Ozgenc Aksoy, A., Arisoy, Y., Guney, M.S., Abdi, V., 2018. Experimental investigation of the equilibrium scour depth below submerged pipes both in live-bed and clear-water regimes under the wave effect. Appl. Ocean Res. 80, 49–56.

Draper, S., An, H., Cheng, L., White, D.J., Griffiths, T., 2015. Stability of subsea pipelines during large storms. Phil. Trans. Math. Phys. Eng. Sci. 373.

Dupuis, A., Chopard, B., 2002. Lattice gas modeling of scour formation under submarine pipelines. J. Comput. Phys. 178, 161–174.

Ehteram, M., Ahmed, A.N., Ling, L., Fai, C.M., Latif, S.D., Afan, H.A., Banadkooki, F.B., EL-Shafie, A., 2020. Pipeline scour rates prediction-based model utilizing a multilayer perceptron-colliding body algorithm. Water (Switzerland) 12, 902.

Etemad-Shahidi, A., Yasa, R., Kazeminezhad, M.H., 2011. Prediction of wave-induced scour depth under submarine pipelines using machine learning approach. Appl. Ocean Res. 33, 54–59.

Ettema, R., Kirkil, G., Muste, M., 2006. Similitude of large-scale turbulence in experiments on local scour at cylinders. J. Hydraul. Eng. 132, 33–40.

Fan, F., Liang, B., Li, Y., Bai, Y., Zhu, Y., Zhu, Z., 2017. Numerical Investigation of the Influence of Water Jumping on the Local Scour beneath a Pipeline under Steady Flow, vol. 9. Water (Switzerland).

Farooq, M., Azhari, F., Banthia, N., 2023. A state-of-the-art review of active-thermometry techniques for bridge and pipeline scour monitoring, and exploratory passive thermometry studies. Journal of Structural Integrity and Maintenance 8, 67–78.

Fredsøe, J., 2016. Pipeline-seabed interaction. J. Waterw. Port, Coast. Ocean Eng. 142, 03116002.

Fredsøe, J., Sumer, B.M., Arnskov, M.M., 1992. Time scale for wave/current scour below pipelines. Int. J. Offshore Polar Eng. 2, 13–17.

Fredsøe, J., Sumer, B.M., Mao, Y., Hansen, E.A., 1988. Three-dimensional scour below pipelines. TRANS. ASME J. OFFSHORE MECH. & ARCT. ENGNG. 110.

Fuhrman, D.R., Baykal, C., Mutlu Sumer, B., Jacobsen, N.G., Fredsøe, J., 2014. Numerical simulation of wave-induced scour and backfilling processes beneath submarine pipelines. Coast Eng. 94, 10–22.

Gao, F.P., Yang, B., Wu, Y.X., Yan, S.M., 2006. Steady current induced seabed scour around a vibrating pipeline. Appl. Ocean Res. 28, 291–298.

Griffiths, T., Draper, S., Sun, W., White, D., Cheng, L., An, H., 2016. Investigation of scour onset under seabed pipelines with geometric irregularities. Scour and Erosion - Proceedings of the 8th International Conference on Scour and Erosion. ICSE, pp. 191–200.

Guan, D., Chiew, Y.M., Wei, M., Hsieh, S.C., 2019a. Visualization of flow field around a vibrating pipeline within an equilibrium scour hole. JoVE 2019, e59745.

Guan, D., Hsieh, S.C., Chiew, Y.M., Low, Y.M., 2019b. Experimental study of scour around a forced vibrating pipeline in quiescent water. Coast Eng. 143, 1–11.

Guan, D., Hsieh, S.C., Chiew, Y.M., Low, Y.M., Wei, M., 2020. Local scour and flow characteristics around pipeline subjected to vortex-induced vibrations. J. Hydraul. Eng. 146, 33560149.

Guan, D.W., Xie, Y.X., Yao, Z.S., Chiew, Y.M., Zhang, J.S., Zheng, J.H., 2022. Local scour at offshore windfarm monopile foundations: a review. Water Sci. Eng. 15, 29–39.
Haghiabi, A.H., 2017. Prediction of river pipeline scour depth using multivariate adaptive regression splines. J. Pipeline Syst. Eng. Pract. 8, 04016015.
Hossein Kazeminezhad, M., Yeganeh-Bakhtiary, A., Etemad-Shahidi, A., Baas, J.H., 2012. Two-phase simulation of wave-induced tunnel scour beneath marine pipelines. J. Hydraul. Eng. 138, 517–529.
Hsu, T.J., Jenkins, J.T., Liu, P.L.F., 2003. On two-phase sediment transport: dilute flow. J. Geophys. Res.: Oceans 108, 1–14.
Hu, D., Tang, W., Sun, L., Li, F., Ji, X., Duan, Z., 2019. Numerical simulation of local scour around two pipelines in tandem using CFD–DEM method. Appl. Ocean Res. 93.
Hu, K., Bai, X., Vaz, M.A., 2023. Numerical simulation on the local scour processing and influencing factors of submarine pipeline. J. Mar. Sci. Eng. 11, 234.
Hu, K., Bai, X., Zhang, Z., Vaz, M.A., 2021. Prediction of submarine pipeline equilibrium scour depth based on machine learning applications considering the flow incident angle. Appl. Ocean Res. 112, 102717.
Hu, R., Wang, X., Liu, H., Leng, H., 2022a. Scour protection of submarine pipelines using ionic soil stabilizer solidified soil. J. Mar. Sci. Eng. 10, 76.
Hu, R., Wang, X., Liu, H., Leng, H., Lu, Y., 2022b. Scour characteristics and equilibrium scour depth prediction around a submarine piggyback pipeline. J. Mar. Sci. Eng. 10, 350.
Huang, J., Yin, G., Ong, M.C., Myrhaug, D., Jia, X., 2021. Numerical investigation of scour beneath pipelines subjected to an oscillatory flow condition. J. Mar. Sci. Eng. 9.
Jabari, V., Masjedi, A., Heidarnejad, M., Kamanbedast, A., Bordbar, A., 2021. Scour control around Submerged pipeline on the river bed using an impermeable Spoiler. Ain Shams Eng. J. 12, 37–45.
Karamzadeh, F., Masjedi, A., Heidarnejad, M., Bordbar, A., 2024. Scour depth analysis beneath a submerged pipeline featuring a protective blade configuration. Results in Engineering 21, 101787.
Karthikeyan, A., Mirza, S., Hur, B., Pearlstein, G., Ledbetter, R., 2020. Quantifying variable importance in predicting critical span length and scour depth for failure of onshore river crossing pipelines using ann. J. Mar. Sci. Eng. 8, 1–18.
Kazeminezhad, M.H., Etemad-Shahidi, A., Yeganeh Bakhtiary, A., 2010. An alternative approach for investigation of the wave-induced scour around pipelines. J. Hydroinf. 12, 51–65.
Kazeminezhad, M.H., Yeganeh-Bakhtiary, A., 2011. Two-phase simulation of coastal current-induced scour around submarine pipelines. J. Coast Res. 542–546.
Kílöz, B., Çevik, E., Yüksel, Y., 2013. Scour below submarine pipelines under irregular wave attack. Coast Eng. 79, 1–8.
Kim, S., Lee, H.J., Yeon, J.H., 2011. Characteristics of parameters for local scour depth around submarine pipelines in waves. Mar. Georesour. Geotechnol. 29, 162–176.
Kizilöz, B., Çevik, E., Aydoğan, B., 2015. Estimation of scour around submarine pipelines with Artificial Neural Network. Appl. Ocean Res. 51, 241–251.
Kjeldsen, S.P., Gjorsvik, O., Bringaker, K., Jacobsen, J., 1973. Local scour near offshore pipelines. 2nd Int. Conf. On Port and Ocean Engineering under Arctic Conditions (POAC). Reykjavik, Iceland.
Kloss, C., Goniva, C., Hager, A., Amberger, S., Pirker, S., 2012. Models, algorithms and validation for opensource DEM and CFD-DEM. Prog. Comput. Fluid Dynam. Int. J. 12, 140–152.
Larsen, B.E., Fuhrman, D.R., Mutlu Sumer, B., 2016. Simulation of wave-plus-current scour beneath submarine pipelines. J. Waterw. Port, Coast. Ocean Eng. 142.
Lee, C.H., 2019. Multi-phase flow modeling of submarine landslides: transformation from hyperconcentrated flows into turbidity currents. Adv. Water Resour. 131, 103383.
Lee, C.H., Huang, Z., 2018. A two-phase flow model for submarine granular flows: with an application to collapse of deeply-submerged granular columns. Adv. Water Resour. 115, 286–300.
Lee, C.H., Low, Y.M., Chiew, Y.M., 2016. Multi-dimensional rheology-based two-phase model for sediment transport and applications to sheet flow and pipeline scour. Phys. Fluids 28.
Lee, C.H., Xu, C., Huang, Z., 2019a. A three-phase flow simulation of local scour caused by a submerged wall jet with a water-air interface. Adv. Water Resour. 129, 373–384.
Lee, J.Y., Forrest, A.L., Hardjanto, F.A., Chai, S., Cossu, R., Leong, Z.Q., 2018. Development of current-induced scour beneath elevated subsea pipelines. J. Ocean Eng. Sci. 3, 265–281.
Lee, J.Y., Hardjanto, F.A., Cossu, R., Chai, S., Leong, Z.Q., Forrest, A.L., 2019b. Current-induced scour beneath initially elevated subsea pipelines. Appl. Ocean Res. 82, 309–324.
Lee, S.O., Sturm, T.W., 2009. Effect of sediment size scaling on physical modeling of bridge pier scour. J. Hydraul. Eng. 135, 793–802.
Li, F., Cheng, L., 1999. Numerical model for local scour under offshore pipelines. J. Hydraul. Eng. 125, 400–406.
Li, F., Cheng, L., 2000. Numerical simulation of pipeline local scour with lee-wake effects. Int. J. Offshore Polar Eng. 10, 195–199.
Li, F.Z., Dwivedi, A., Low, Y.M., Hong, J.H., Chiew, Y.M., 2013. Experimental investigation on scour under a vibrating catenary riser. J. Eng. Mech. 139, 868–878.
Li, H., Wang, S., Chen, X., Hu, C., Liu, J., 2021a. Numerical study of scour depth effect on wave-induced seabed response and liquefaction around a pipeline. Mar. Georesour. Geotechnol. 39, 188–199.
Li, X., Hu, Y., Han, Z., 2023. Fatigue condition assessment of subsea pipelines under vortex induced vibration and cyclical lateral displacement. Energy Sources, Part A Recovery, Util. Environ. Eff. 45, 9941–9957.
Li, X., Zhang, Y., Abbassi, R., Khan, F., Chen, G., 2021b. Probabilistic fatigue failure assessment of free spanning subsea pipeline using dynamic Bayesian network. Ocean Eng. 234, 109323.
Li, Y., Ong, M.C., Fuhrman, D.R., 2020a. CFD investigations of scour beneath a submarine pipeline with the effect of upward seepage. Coast Eng. 156, 103624.
Li, Y., Ong, M.C., Fuhrman, D.R., Larsen, B.E., 2020b. Numerical investigation of wave-plus-current induced scour beneath two submarine pipelines in tandem. Coast Eng. 156.
Liang, B., DU, S., Pan, X., Zhang, L., 2020. Local scour for vertical piles in steady currents: review of mechanisms, influencing factors and empirical equations. J. Mar. Sci. Eng. 8, 4.
Liang, D., Cheng, L., 2005. Numerical model for wave-induced scour below a submarine pipeline. J. Waterw. Port, Coast. Ocean Eng. 131, 193–202.
Liang, D., Cheng, L., Li, F., 2005a. Numerical modeling of flow and scour below a pipeline in currents. Part II. Scour simulation. Coast Eng. 52, 43–62.
Liang, D., Cheng, L., Yeow, K., 2005b. Numerical study of the Reynolds-number dependence of two-dimensional scour beneath offshore pipelines in steady currents. Ocean Eng. 32, 1590–1607.
Liang, D., Huang, J., Zhang, J., Shi, S., Zhu, N., Chen, J., 2022. Three-dimensional simulations of scour around pipelines of finite lengths. J. Mar. Sci. Eng. 10.
Liang, D., Li, T., Xiao, Y., 2016. Simulation of scour around a vibrating pipe in steady currents. J. Hydraul. Eng. 142, 04015049.
Liang, W., Lou, M., Fan, C., Zhao, D., Li, X., 2023. Coupling effect of vortex-induced vibration and local scour of double tandem pipelines in steady current. Ocean Eng. 286, 115495.
Liu, K.W., Jiang, N.J., Qin, J.D., Wang, Y.J., Tang, C.S., Han, X.L., 2021a. An experimental study of mitigating coastal sand dune erosion by microbial- and enzymatic-induced carbonate precipitation. Acta Geotechnica 16, 467–480.
Liu, M., Tang, G., Zhang, Q., Jin, X., 2023. Numerical investigate of the effects of surface roughness on local scour around pipeline under steady current condition. Ocean Eng. 290, 116077.
Liu, M.M., 2021. Numerical investigation of local scour around submerged pipeline in shoaling conditions. Ocean Eng. 234.
Liu, M.M., Jin, X., Wang, L., Yang, F., Tang, J., 2021b. Numerical investigation of local scour around a vibrating pipeline under steady currents. Ocean Eng. 221.
Liu, M.M., Lu, L., Teng, B., Zhao, M., Tang, G.Q., 2016. Numerical modeling of local scour and forces for submarine pipeline under surface waves. Coast Eng. 116, 275–288.
Lu, L., Li, Y., Qin, J., 2005. Numerical simulation of the equilibrium profile of local scour around submarine pipelines based on renormalized group turbulence model. Ocean Eng. 32, 2007–2019.
Luan, Y., Liang, D., Rana, R., 2015. Scour depth beneath a pipeline undergoing forced vibration. Theoret. Appl. Mech. Letters 5, 97–100.
Luo, C., An, H., Cheng, L., White, D., 2014. A model for predicting pipeline sinkage induced by tunnel scour. Geotech. Eng. 45, 46–52.
Ma, H., Li, B., 2023. CFD-CGDEM coupling model for scour process simulation of submarine pipelines. Ocean Eng. 271, 113789.
Ma, H., Li, B., Zhang, S., 2024. Scour mechanism around a pipeline under different current-wave conditions using the CFD-DEM coupling model. Comput. Geotech. 170.
Mathieu, A., Chauchat, J., Bonamy, C., Nagel, T., 2019. Two-phase flow simulation of tunnel and lee-wake erosion of scour below a submarine pipeline. Water (Switzerland) 11.
Ming-Ming, L., Hao-Cheng, W., Fei-Fei, S., Xin, J., Guo-Qiang, T., Fan, Y., 2022. Numerical investigation of local scour around a vibration pipeline under free surface wave condition. Ocean Eng. 245.
Mohr, H., Draper, S., Cheng, L., White, D.J., 2016. Predicting the rate of scour beneath subsea pipelines in marine sediments under steady flow conditions. Coast Eng. 110, 111–126.
Moncada, A.T.M., Aguirre-Pe, J., 1999. Scour below pipeline in river crossings. J. Hydraul. Eng. 125, 953–958.
Mousavi, M.E., Bakhtiary, A.Y., Enshaei, N., 2009. The equivalent depth of wave-induced scour around offshore pipelines. J. Offshore Mech. Arctic Eng. 131, 1–5.
Myrhaug, D., Ong, M.C., 2021. Time scale for scour beneath pipelines due to long-crested and short-crested nonlinear random waves plus current. J. Mar. Sci. Eng. 9, 1–11.
Myrhaug, D., Ong, M.C., Føien, H., Gjengedal, C., Leira, B.J., 2009. Scour below pipelines and around vertical piles due to second-order random waves plus a current. Ocean Eng. 36, 605–616.
Myrhaug, D., Ong, M.C., Gjengedal, C., 2008. Scour below marine pipelines in shoaling conditions for random waves. Coast Eng. 55, 1219–1223.
Najafzadeh, M., Barani, G.A., Azamathulla, H.M., 2014a. Prediction of pipeline scour depth in clear-water and live-bed conditions using group method of data handling. Neural Comput. Appl. 24, 629–635.
Najafzadeh, M., Barani, G.A., Hessami Kermani, M.R., 2014b. Estimation of pipeline scour due to waves by GMDH. J. Pipeline Syst. Eng. Pract. 5, 06014002.
Najafzadeh, M., Oliveto, G., 2021. Exploring 3D wave-induced scouring patterns around subsea pipelines with artificial intelligence techniques. Appl. Sci. 11, 3792.
Najafzadeh, M., Oliveto, G., 2022. Scour propagation rates around offshore pipelines exposed to currents by applying data-driven models. Water (Switzerland) 14, 493.
Najafzadeh, M., Oliveto, G., Saberi-Movahed, F., 2022. Estimation of scour propagation rates around pipelines while considering simultaneous effects of waves and currents conditions. Water (Switzerland) 14, 1589.
Najafzadeh, M., Saberi-Movahed, F., 2019. GMDH-GEP to predict free span expansion rates below pipelines under waves. Mar. Georesour. Geotechnol. 37, 375–392.
Najafzadeh, M., Sarkamaryan, S., 2018. Extraction of optimal equations for evaluation of pipeline scour depth due to currents. Proc. Inst. Civ. Eng.: Maritime Eng. 171, 1–10.
Ouyang, H., Dai, G., Gao, L., Zhu, W., DU, S., Gong, W., 2022. Local scour characteristics of monopile foundation and scour protection of cement-improved soil in marine environment - laboratory and site investigation. Ocean Eng. 255, 111443.

Parchure, T.M., Mehta, A.J., 1985. Erosion of soft cohesive sediment deposits. J. Hydraul. Eng. 111, 1308–1326.
Parsaie, A., Haghiabi, A.H., Moradinejad, A., 2019. Prediction of scour depth below river pipeline using support vector machine. KSCE J. Civ. Eng. 23, 2503–2513.
Petersen, T.U., Mutlu Sumer, B., Fredsøe, J., Raaijmakers, T.C., Schouten, J.J., 2015. Edge scour at scour protections around piles in the marine environment - laboratory and field investigation. Coast Eng. 106, 42–72.
Postacchini, M., Brocchini, M., 2015. Scour depth under pipelines placed on weakly cohesive soils. Appl. Ocean Res. 52, 73–79.
Qu, L., An, H., Draper, S., Watson, P., Zhao, M., Harris, J., Whitehouse, R., Zhang, D., 2024. A review of scour impacting monopiles for offshore wind. Ocean Eng. 301.
Rodríguez, I., Lehmkuhl, O., Chiva, J., Borrell, R., Oliva, A., 2015. On the flow past a circular cylinder from critical to super-critical Reynolds numbers: wake topology and vortex shedding. Int. J. Heat Fluid Flow 55, 91–103.
Salehi, S., Azimi, A.H., 2022. Effects of spoiler and piggyback on local scour under single and twin submerged pipes. Ocean Eng. 261, 112137.
Serta Fraga, V., Yin, G., Ong, M.C., Myrhaug, D., 2022. CFD investigation on scour beneath different configurations of piggyback pipelines under steady current flow. Coast Eng. 172.
Sharafati, A., Tafarojnoruz, A., Motta, D., Yaseen, Z.M., 2020. Application of nature-inspired optimization algorithms to ANFIS model to predict wave-induced scour depth around pipelines. J. Hydroinf. 22, 1425–1451.
Sharafati, A., Yasa, R., Azamathulla, H.M., 2018. Assessment of stochastic approaches in prediction of wave-induced pipeline scour depth. J. Pipeline Syst. Eng. Pract. 9, 04018024.
Shi, Y., Yang, H., Wei, J., Yu, H., Liu, Y., Ge, S., Bai, Z., Li, S., 2022. Numerical study of scour below vibrating pipelines under waves and currents. Ocean Eng. 266, 112718.
Song, S., Park, S., 2022. Unresolved CFD and DEM coupled simulations on scour around a subsea pipeline. J. Mar. Sci. Eng. 10, 556.
Soulsby, R.L., 1997. Dynamics of Marine Sands. Thomas Telford.
Subiyanto & Tofany, N., 2024. Numerical simulation of pipeline scour and sedimentation around submerged pipelines with an open-source multiphase-CFD model. CFD Lett. 16, 150–165.
Sui, T., Staunstrup, L.H., Carstensen, S., Fuhrman, D.R., 2021. Span shoulder migration in three-dimensional current-induced scour beneath submerged pipelines. Coast Eng. 164, 103776.
Sumer, B.M., Fredsøe, J., 1990. Scour below pipelines in waves. J. Waterw. Port, Coast. Ocean Eng. 116, 307–323.
Sumer, B.M., Fredsøe, J., 1996. Scour around pipelines in combined waves and current. Proceedings of the International Conference on Offshore Mechanics and Arctic Engineering -. OMAE, pp. 595–602.
Sumer, B.M., Fredsøe, J., 2002. The mechanics of scour in the marine environment. In: Advanced Series on Ocean Engineering, 17. World Scientific.
Sumer, B.M., Fredsøe, J., 2006. Hydrodynamics Around Cylindrical Structures (Revised Edition). World Scientific.
Sumer, B.M., Fredsøe, J., Gravesen, H., Bruschi, R., 1989. Response of marine pipelines in scour trenches. J. Waterw. Port, Coast. Ocean Eng. 115, 477–496.
Sumer, B.M., Jensen, H.R., Fredsoe, J., Mao, Y., 1988a. Effect of lee-Wake on scour below pipelines in current. J. Waterway Port Coast. Ocean. Eng. (ASCE) 114, 599–614.
Sumer, B.M., Mao, Y., Fredsøe, J., 1988b. Interaction between vibrating pipe and erodible bed. J. Waterw. Port, Coast. Ocean Eng. 114, 81–92.
Sumer, B.M., Truelsen, C., Sichmann, T., Fredsøe, J., 2001. Onset of scour below pipelines and self-burial. Coast Eng. 42, 313–335.
Tafarojnoruz, A., Gaudio, R., Dey, S., 2010. Flow-altering countermeasures against scour at bridge piers: a review. J. Hydraul. Res. 48, 441–452.
Tofany, N., Low, Y.M., Lee, C.H., Chiew, Y.M., 2019. Two-phase flow simulation of scour beneath a vibrating pipeline during the tunnel erosion stage. Phys. Fluids 31.
Tofany, N., Putra, D.E., Latifah, A.L., 2023. Current-induced scouring around a submarine pipeline using a multi-phase flow model with different inter-phase drag models. Ocean Eng. 286, 115691.
Tofany, N., Wirahman, T., 2022. Numerical simulation of early stages of scour around a submarine pipeline using a two-phase flow model. Ocean Eng. 264, 112503.
Tom, J.G., Draper, S., White, D.J., 2018. Sediment transport and trench development beneath a cylinder oscillating normal to a sandy seabed. Coast Eng. 140, 395–410.
Tsai, B., Mathieu, A., Montellà, E.P., Hsu, T.J., Chauchat, J., 2022. An Eulerian two-phase flow model investigation on scour onset and backfill of a 2D pipeline. Eur. J. Mech. B Fluid 91, 10–26.
Van Prooijen, B.C., Winterwerp, J.C., 2010. A stochastic formulation for erosion of cohesive sediments. J. Geophys. Res.: Oceans 115, C01005.
Vijaya Kumar, A., Neelamani, S., Narasimha Rao, S., 2002. Wave pressures and uplift forces on and scour around submarine pipeline in clayey soil. Ocean Eng. 30, 271–295.
Vosoughi, H., Hajikandi, H., 2020. Scour around submarine pipes due to high-amplitude transient waves. Water Sci. Eng. 13, 154–161.
Wang, W., Yan, J., Chen, S., Liu, J., Jin, F., Wang, B., 2023. Gridded cemented riprap for scour protection around monopile in the marine environment. Ocean Eng. 272, 113876.
Williamson, C.H.K., Roshko, A., 1988. Vortex formation in the wake of an oscillating cylinder. J. Fluid Struct. 2, 355–381.
Wu, X., Li, R., Shu, J., Chen, J., Wang, H., Jiang, H., Wang, X., 2024. Anti-scour performance of fluidized solidified slurry in dynamic water for scour repair. Ocean Eng. 291.
Wu, Y., Chiew, Y.M., 2012. Three-dimensional scour at submarine pipelines. J. Hydraul. Eng. 138, 788–795.
Wu, Y., Chiew, Y.M., 2013. Mechanics of three-dimensional pipeline scour in unidirectional steady current. J. Pipeline Syst. Eng. Pract. 4, 3–10.
Wu, Y., Chiew, Y.M., 2015. Mechanics of pipeline scour propagation in the spanwise direction. J. Waterw. Port, Coast. Ocean Eng. 141.
Xie, L., Zhu, Y., Su, T.C., 2019a. Scour protection of partially embedded pipelines using sloping curtains. J. Hydraul. Eng. 145, 04019001.
Xie, L., Zhu, Y., Su, T.C., 2019b. Visualization tests on variation of scour front under a pipeline in steady currents. J. Mar. Sci. Eng. 7, 345.
Yan, X., Mohammadian, A., Rennie, C.D., 2020. Numerical modeling of flow and local scour around pipeline in steady currents using moving mesh with masked elements. J. Hydraul. Eng. 146.
Yang, B., Liang, B., Zhang, Q., Zhao, M., Qu, M., 2024. Numerical investigation of flow around the sagging pipeline above an equilibrium scoured bed. Ocean Eng. 311, 118785.
Yang, B., Yang, T., Ma, J.L., Cui, J.S., 2013. The experimental study on local scour around a circular pipe undergoing vortex-induced vibration in steady flow. J. Mar. Sci. Technol. 21, 250–257.
Yang, J., Low, Y.M., Lee, C.H., Chiew, Y.M., 2018. Numerical simulation of scour around a submarine pipeline using computational fluid dynamics and discrete element method. Appl. Math. Model. 55, 400–416.
Yang, L., Guo, Y., Shi, B., Kuang, C., Xu, W., Cao, S., 2012a. Study of scour around submarine pipeline with a rubber plate or rigid spoiler in wave conditions. J. Waterw. Port, Coast. Ocean Eng. 138, 484–490.
Yang, L., Shi, B., Guo, Y., Wen, X., 2012b. Calculation and experiment on scour depth for submarine pipeline with a spoiler. Ocean Eng. 55, 191–198.
Yang, L., Shi, B., Guo, Y., Zhang, L., Zhang, J., Han, Y., 2014. Scour protection of submarine pipelines using rubber plates underneath the pipes. Ocean Eng. 84, 176–182.
Yang, S., Guo, Y., Shi, B., Yu, G., Yang, L., Zhang, M., 2021. Numerical investigation of the influence of the small pipeline on local scour morphology around the piggyback pipeline. Ocean Eng. 240, 109973.
Yang, S., Shi, B., Guo, Y., 2019. Investigation on scour scale of piggyback pipeline under wave conditions. Ocean Eng. 182, 196–202.
Yasa, R., Etemad-Shahidi, A., 2013. Classification and regression trees approach for predicting current-induced scour depth under pipelines. J. Offshore Mech. Arctic Eng. 136.
Yeganeh-Bakhtiary, A., Zanganeh, M., Kazemi, E., Cheng, L., Abd Wahab, A.K., 2013. Euler-Lagrange two-phase model for simulating live-bed scour beneath marine pipelines. J. Offshore Mech. Arctic Eng. 135, 31705, 1.
Zang, Z., Chen, Y., Zhang, J., Tian, Y., Esteban, M.D., 2021. Experimental study on local scour and onset of VIV of a pipeline on a silty seabed under steady currents. Appl. Ocean Res. 109.
Zang, Z., Cheng, L., Zhao, M., Liang, D., Teng, B., 2009. A numerical model for onset of scour below offshore pipelines. Coast Eng. 56, 458–466.
Zang, Z., Tang, G., Chen, Y., Cheng, L., Zhang, J., 2019. Predictions of the equilibrium depth and time scale of local scour below a partially buried pipeline under oblique currents and waves. Coast Eng. 150, 94–107.
Zang, Z., Zhao, M., Chen, E., Zhang, Q., 2024. Numerical modeling of local scour around a subsea pipeline on cohesive seabed under steady currents. Mar. Georesour. Geotechnol.
Zanganeh, M., Yeganeh-Bakhtiary, A., Abd Wahab, A.K., 2012. Lagrangian coupling two-phase flow model to simulate current-induced scour beneath marine pipelines. Appl. Ocean Res. 38, 64–73.
Zhai, H., Jeng, D.S., 2024. Impacts of wave-induced seabed response on local scour around a pipeline: poro–fssi–scour–foam. Coast Eng. 187, 104424.
Zhang, F., Zang, Z., Zhao, M., Zhang, J., Xie, B., Zou, X., 2022a. Numerical investigations on scour and flow around two crossing pipelines on a sandy seabed. J. Mar. Sci. Eng. 10, 2019.
Zhang, Q., Draper, S., Cheng, L., An, H., 2016a. Effect of limited sediment supply on sedimentation and the onset of tunnel scour below subsea pipelines. Coast Eng. 116, 103–117.
Zhang, Q., Draper, S., Cheng, L., An, H., 2016b. Scour below a subsea pipeline in time varying flow conditions. Appl. Ocean Res. 55, 151–162.
Zhang, Q., Draper, S., Cheng, L., An, H., 2017a. Time scale of local scour around pipelines in current, waves, and combined waves and current. J. Hydraul. Eng. 143, 1750002.
Zhang, Q., Draper, S., Cheng, L., Zhao, M., An, H., 2017b. Experimental study of local scour beneath two tandem pipelines in steady current. Coast Eng. J. 59.
Zhang, Q., Zhou, X.L., Wang, J.H., Li, W.L., 2019a. Dynamic interaction between two parallel submarine pipelines considered vortex-induced vibration and local scour. Mar. Georesour. Geotechnol. 37, 609–621.
Zhang, Q., Zhou, X.L., Xia, X.H., Li, W.L., Zhang, S., 2019b. Coupling effect of vortex-induced vibration of a submarine pipeline and local scour under steady current. J. Offshore Mech. Arctic Eng. 141, 041702.
Zhang, Y., Wu, J., Zhang, S., Li, G., Jeng, D.S., Xu, J., Tian, Z., Xu, X., 2022b. An optimal statistical regression model for predicting wave-induced equilibrium scour depth in sandy and silty seabeds beneath pipelines. Ocean Eng. 258, 111709.
Zhang, Y., Zhang, S., Li, G., 2019c. Seabed scour beneath an unburied pipeline under regular waves. Mar. Georesour. Geotechnol. 37, 1247–1256.
Zhang, Y., Zhao, M., Kwok, K.C.S., Liu, M.M., 2014. Computational fluid dynamics-discrete element method analysis of the onset of scour around subsea pipelines. Appl. Math. Model. 39, 7611–7619.
Zhang, Z., Chiew, Y.M., Ji, C., 2022c. Experimental study on local scour around a forced vibrating pipeline in unidirectional flows. Coast Eng. 176.
Zhang, Z., Chiew, Y.M., Ji, C., 2023. Equilibrium depth and time scale of local scour around a forced vibrating pipeline. Coast Eng. 185, 104378.

Zhang, Z., Guo, Y., Yang, Y., Shi, B., Wu, X., 2021. Scale model experiment on local scour around submarine pipelines under bidirectional tidal currents. J. Mar. Sci. Eng. 9, 1421.
Zhang, Z., Shi, B., 2016. Numerical simulation of local scour around underwater pipeline based on FLUENT software. J. Appl. Fluid Mech. 9, 711–718.
Zhao, E., Dong, Y., Tang, Y., Sun, J., 2021. Numerical investigation of hydrodynamic characteristics and local scour mechanism around submarine pipelines under joint effect of solitary waves and currents. Ocean Eng. 222.
Zhao, E., Shi, B., Qu, K., Dong, W., Zhang, J., 2018. Experimental and numerical investigation of local scour around submarine piggyback pipeline under steady current. J. Ocean Univ. China 17, 244–256.
Zhao, M., 2022. A review on recent development of numerical modelling of local scour around hydraulic and marine structures. J. Mar. Sci. Eng. 10.
Zhao, M., 2023. A review of recent studies on the control of vortex-induced vibration of circular cylinders. Ocean Eng. 285, 115389.
Zhao, M., Cheng, L., 2008. Numerical modeling of local scour below a piggyback pipeline in currents. J. Hydraul. Eng. 134, 1452–1463.
Zhao, M., Cheng, L., 2010. Numerical investigation of local scour below a vibrating pipeline under steady currents. Coast Eng. 57, 397–406.
Zhao, M., Cheng, L., Teng, B., 2007. Numerical modeling of flow and hydrodynamic forces around a piggyback pipeline near the seabed. J. Waterw. Port, Coast. Ocean Eng. 133, 286–295.
Zhao, M., Vaidya, S., Zhang, Q., Cheng, L., 2015a. Local scour around two pipelines in tandem in steady current. Coast Eng. 98, 1–15.
Zhao, X., Ba, Q., Zhou, L., Li, W., Ou, J., 2014. BP neural network recognition algorithm for scour monitoring of subsea pipelines based on active thermometry. Optik 125, 5426–5431.
Zhao, X., Li, W., Song, G., Zhu, Z., DU, J., 2013. Scour monitoring system for subsea pipeline based on active thermometry: numerical and experimental studies. Sensors 13, 1490–1509.
Zhao, X., Li, W., Zhou, L., Song, G., Ba, Q., Ho, S.C.M., Ou, J., 2015b. Application of support vector machine for pattern classification of active thermometry-based pipeline scour monitoring. Struct. Control Health Monit. 22, 903–918.
Zhao, X., Zhao, M., Cheng, L., 2011. Numerical investigation of scale effects in modelling scour below offshore pipelines under steady currents. Proceedings of the International Conference on Offshore Mechanics and Arctic Engineering -. OMAE, pp. 931–938.
Zhao, X.F., Ba, Q., Li, L., Gong, P., Ou, J.P., 2012a. A three-index estimator based on active thermometry and a novel monitoring system of scour under submarine pipelines. Sens. Actuators, A 183, 115–122.
Zhao, X.F., Li, L., Ba, Q., Ou, J.P., 2012b. Scour monitoring system of subsea pipeline using distributed Brillouin optical sensors based on active thermometry. Opt Laser. Technol. 44, 2125–2129.
Zhao, Z., Fernando, H.J.S., 2007. Numerical simulation of scour around pipelines using an Euler - euler coupled two-phase model. Environ. Fluid Mech. 7, 121–142.
Zhou, C., Li, J., Wang, J., Tang, G., 2021. Numerical study of local scour around a submarine pipeline with a spoiler using a symmetry boundary condition. Symmetry 13.
Zhu, H., Qi, X., Lin, P., Yang, Y., 2013. Numerical simulation of flow around a submarine pipe with a spoiler and current-induced scour beneath the pipe. Appl. Ocean Res. 41, 87–100.
Zhu, L., Liu, K., Fan, H., Cao, S., Chen, H., Wang, J., Wang, Z., 2019. Scour beneath and adjacent to submarine pipelines with spoilers on a cohesive seabed: case study of Hangzhou Bay, China. J. Waterw. Port, Coast. Ocean Eng. 145, 05018009.
Zhu, Y., Xie, L., Su, T.C., 2020a. Scour protection effects of a geotextile mattress with floating plate on a pipeline. Sustainability 12, 3482.
Zhu, Y., Xie, L., Wong, T., Su, T.C., 2022. Development of three-dimensional scour below pipelines in regular waves. J. Mar. Sci. Eng. 10, 124.
Zhu, Y., Xie, L., Wong, T.M., Su, T.C., 2020b. Visualization of the onset of scour under a pipeline in waves. Appl. Sci. 10, 2994.